Laboratory Perspectives on the Chemical Transformations of Organic Matter in Atmospheric Particles

Yinon Rudich

Department of Environmental Sciences, Weizmann Institute, Rehovot 76100, Israel

Received February 3, 2003

Contents

[Throughout the text, selected words and phrases are marked with †. These terms are defined in detail in the Glossary (section 8).]

Yinon Rudich received his B.Sc. degree from Ben Gurion University and M.Sc. and Ph.D. degrees in chemistry from the Weizmann Institute. Following postdoctoral work with A. R. Ravishankara at the National Oceanic and Atmospheric Administration in Boulder, he joined the Weizmann Institute of Science, where he is presently a Professor of Chemistry at the Department of Environmental Sciences and Energy Research. His research interests include the chemistry of organic aerosols and of mineral dust, aerosol–climate interactions, and characterization of ambient atmospheric aerosols. Other interests include heterogeneous atmospheric chemistry and development of new analytical techniques for characterization of atmospheric particles.

> *I had, when a youth, read and smiled at Pliny's account of a practice among the seamen of his time, to still the waves in a storm by pouring oil into the sea; which he mentions as well as the use made of oil by the divers; but the stilling a tempest by throwing vinegar into the air had escaped me. I think that it has been of late too much the mode to slight the learning of the ancients. The learned, too, are apt to slight too much the knowledge of the vulgar. The cooling by evaporation was long an instance of the latter. The art of smoothing the waves by oil is an instance of both.*
>
> From a letter sent by Benjamin Franklin to William Brownrigg, 1773

1. Introduction

People have long ago discovered the effects of oil on the surface properties of water.[1,2] Lisbon seamen dropped oil from their boats to suppress the breakers when they returned to the harbor. Bermudan divers used to spread oil on the surface of the water to

10.1021/cr020508f CCC: $44.00 © 2003 American Chemical Society
Published on Web 08/29/2003

enable penetration of light to the depths, and the port of Newport (Rhode Island) always had calm waters while the whaling vessels were docked. In a famous experiment, Benjamin Franklin spread a teaspoon of oil over a lake in Calpham's common and noticed that the oil spread dramatically, forming a film so thin that it produced what he termed "prismatic colors". In light of these early observations of the effects of oils on water surfaces, it is no surprise that the effects of organic compounds on the properties of atmospheric aerosols and cloud droplets are so significant and are the focus of modern research in atmospheric chemistry.

1.1. Climatic and Environmental Effects of Organic Aerosols

Aerosols play major roles in environmental issues related to global and regional climate, chemistry of the atmosphere, the hydrological cycle, and people's health.[3−8] Aerosols influence the climate directly by changing radiative forcing through absorption and scattering of incoming solar radiation. Aerosols also affect the climate indirectly via the modification of cloud properties such as cloud cover, reflectance, ability to precipitate, vertical extent and lifetime.[9] The direct and indirect climatic effects of particles are amongst the largest uncertainties in current climate research.[10] Heterogeneous and multiphase† processes involving aerosols also affect the chemistry of the atmosphere.[7,11,12] Lastly, aerosols also affect the health and well being of humans via inhalation of small size particles.[13−16]

It was recently recognized that the organic matter is a major component of atmospheric aerosols and is ubiquitous in the atmosphere.[3,17,18] Organic matter dramatically affects the development of cloud droplets through modification of surface tension and of mass transfer into and out of the droplets.[19−21] Therefore, dissolved and surface-active organic compounds in droplets and aerosols can lead to formation of smaller droplets and hence directly affect the albedo† of clouds and rain development.[19,20,22,23] The amount of water-soluble and insoluble organic material in particles affects their ability to nucleate cloud droplets.[24] The organic aerosol component also affects climate via scattering and absorption of incoming solar radiation. These phenomena are currently not well characterized.[3,9,25] The combination of scattering of incoming solar radiation by organic aerosols and strong absorption of light by black carbon significantly reduces the amount of solar energy reaching the surface.[5,6,8] Heating of the atmospheric region where absorbing aerosols reside can lead to several dynamical effects, such as stabilization of the atmosphere below and inducing a region of instability above the absorbing layer. These climatic and dynamics effects lead to regional effects on the hydrological cycle.[26]

Among the main challenges in modern climate research is the need to unravel the linkages among aerosols, cloud formation, and climate change and the specific role that organic material plays in these processes. Unraveling this complex linkage must start by relating the processes at the microscopic level of aerosol formation and transformation with larger scale chemical and cloud physical processes.[27]

1.2. Sources of Organic Matter in Aerosols

The term "organic aerosols" is commonly used to describe aerosols that have a substantial organic component. Most atmospheric particles, however, contain both organic and inorganic components. To follow everyday notion, we will use the term "organic aerosol" in this article.

Organic aerosol components have primary sources such as wax emissions from vegetation, combustion, biomass burning, or sea spray carrying organic material from the ocean's surface. Alternatively, organic aerosol can form *in-situ* by photochemical oxidation reactions of gas-phase trace species which yield low-vapor-pressure oxygenated compounds that condense on existing airborne particles (secondary sources).[28−30] The relative contributions of these two source processes depend on the local types of emissions as well as on the meteorological and atmospheric chemical conditions. Despite major analytical efforts, the exact chemical composition of organic aerosols is not well characterized.[3,31,32] Nor are the phase of the particles and the amount of mixing with inorganic species known. Organic matter in aerosols can be found both as solid matter and as viscous fluids,[33] as coatings over an inorganic core, or internally mixed with inorganic compounds.[19,21,34−39] Most of the organic compounds found in aerosols are low-vapor-pressure species, usually polyaromatic hydrocarbons (PAH), dicarboxylic organic acids, or highly oxygenated, multifunctional compounds.[40] Organic compounds compose a major fraction of fine ($<1\ \mu$m) aerosols, where they are the second most abundant component after sulfates.[3] They can also be found on super micron particles such as the coarse fraction of biomass burning aerosols, on sea salt aerosols, and adsorbed on mineral dust particles.

1.3. Organic Compounds on Surfaces of Droplets and Aerosols

Surface-active humic-like substances were found in cloud and fog droplets.[41] The source of the humic substance is not completely clear, although there is an indication that it may form *in-situ* by a series of chemical reactions, or originate either from the soil or from biomass combustion.[42,43] Sea salt aerosol coated by organics in form of inverted micelle†-like films forms by wave action.[35] The organic film is probably made of large hydrocarbons, which are possibly the products of lipid membrane degradation.[38,39,44] Surface tension measurements suggest that atmospheric water droplets could also be coated by an organic layer.[45] Organic-coated particles from marine sources were identified by scanning electron microscopy (SEM) coupled with an energy dispersive X-ray microanalyzer (EDX)†[38] and by mass spectrometric techniques.[39] Inorganic particles encapsulated by an organic coating were also observed by atomic force microscopy and electron microscopy.[46] However, these methods do not reveal information about the chemical composition of the organic films. Organic

functional groups (aromatic, alkyl, ketonic carbonyl, and carboxylic carbonyl groups) were identified in individual dry particles with diameters ranging from 0.2 to 10 μm showing regions of different compositions within particles.[37] The organic material on the surface was found to be enriched in shorter chain compounds and oxygenated groups, indicating the presence of surface-active carboxylic acids.[37] Organic compounds such as PAH, pesticides, and carboxylic acids were also identified on the surface of mineral dust particles.[47]

1.4. Chemical Modifications of Organic Films and Coated Particles

Due to interactions with oxidizing species present in the atmosphere, particle-associated organic matter undergoes constant changes during its atmospheric residence time. Nonreactive uptake of water and additional organic and inorganic trace gases, as well as reactions with atmospheric oxidants, constantly modifies the properties of organic aerosols. The environmental impacts of aerosol-bound compounds, such as pesticides, will be determined by chemical reactions on the surfaces and in the bulk of aerosols.[48] Changes in the aerosols' chemical and physical properties dictate how the particles participate in the various environmental processes. Reliable modeling of organic aerosols and accurate assessment of their influence on the Earth system must include a detailed understanding of heterogeneous and multiphase chemical processes.[11] Yet many of the important processes are still not well characterized.[4,7,11,49] Specifically, many parameters such as reactive and nonreactive uptake coefficients† as well as reaction mechanisms, products identification and yields that are required for modeling the chemistry and physics of organic aerosols, are still generally unknown. This gap in knowledge sparked an intense effort to study the properties and chemistry of organic aerosols.

1.5. Scope of this Review

The scope of this review will be limited to a literature survey of current laboratory studies, illustrating the "state of the science" with regard to physical and chemical processes of organic aerosols. These studies aim at understanding how chemical processes of the organic matter affect aerosol properties from the chemical, kinetic, and mechanistic points of view. As a result, the term "organic aerosols" will be used as a wide definition which includes particles with high organic content or particles with surface-active organic coatings. Different experimental approaches used for these studies will be explored, and the properties and questions that each addresses will be presented. The next sections will describe processes which have been addressed in laboratory studies, including determination of uptake coefficients (reactive and nonreactive) by kinetic techniques, effects of organic matter on water adsorption† onto aerosols' surfaces, and reaction mechanisms for gas-particle interactions. This review will focus on the chemistry of the organic components of aerosols and will describe laboratory studies that use well-defined model systems for organic aerosols. The focus will be organic carbon that is either emitted directly by processes such as combustion, biomass burning, or wave action or formed by atmospheric photochemical processes and is incorporated into atmospheric particles.

Explicitly, this review will not cover studies of soot and black carbon despite their important climatic and environmental effects.[6,25,50] Studies that focus on the chemical and physical mechanisms leading to organic aerosols formation (see examples in refs 19 and 51−59) or studies of uptake of organics by aqueous aerosols, mineral dust, or acids (see examples in refs 60−63) will also not be covered. Generally, these topics are considered separate areas of research and will be subject to separate reviews.

2. Model Systems for Organic Aerosols

Atmospheric aerosols contain a wide range of different organic species with diverse functional groups.[31,64,65] Therefore, it is not practical to study each of the species. Consequently, a number of model systems, also known as proxies, have been developed for laboratory experiments. These model systems represent one or more aspects of atmospheric particles, and they vary in their complexity and in how much they represent the real environmental matrix. The assumptions for using each one of these models should be kept in mind when deriving conclusions and when making extrapolations from the laboratory systems to the atmosphere. In this section the models used in various studies will be described. Some of the experimental apparatuses that have been used for such studies will also be presented. This section will begin with the most "idealized" proxy, organic monolayers, and will proceed to more complex and realistic systems, such as aerosols in photochemical reactors. Most of the different experimental techniques have been described in detail in previous publications;[66−79] therefore, the readers are referred to these publications for an in-depth description.

Because of the large diversity of the organic compounds and the need to include them in meaningful ways in models, Fuzzi et al.[80] derived a simplified model of the water soluble organic fraction of atmospheric aerosols using nuclear magnetic (NMR) spectroscopy. Using quantitative measurements of the organic carbon and the concentrations of the main functional groups composing the aerosol water soluble organic compounds (WSOC), a set of a few model compounds are obtained. These model mixtures are thought to represent the chemical and physical properties of aerosol WSOC and therefore may be useful in future model studies. Using infrared spectroscopy, Maria et al.[81] identified the major functional groups of organic matter in collected particles. By combining the spectroscopic measurements with solvent extraction methods, it was possible to separate these functional groups into fractions of increasing hygroscopicity. This method provides chemical information about the composition of organics in aerosols, which may be used to devise realistic models for laboratory studies.

2.1. Monolayer Organic Films

Surfaces of organic aerosols are constantly modified by interactions with gas-phase oxidants and radicals as well as with atmospheric water vapor. Therefore, surface chemistry will determine to a large extent the environmental roles played by particles. To address the questions of surface processes and the need to separate between surface and bulk processes, organic monolayers were introduced to research in atmospheric chemistry. While the properties and chemistry of organic monolayers have been a subject of intense research in physical chemistry and material sciences (see, for example, in ref 82), they have been introduced to atmospheric chemistry research only recently. The effects of chemical properties such as chain length, surface corrugation, and the presence of double bonds on reactivity were studied. More chemically complex monolayers have not yet been used, mostly due to the synthetic challenges which they require.

Organic monolayers are ideal surfaces for laboratory experiments: they are well-ordered, have well-defined geometry, and can be well characterized before and after reaction. Although the organic surfaces studied in the laboratory are very different from the surfaces of real atmospheric particles, they enabled researchers to probe the reactive processes that are confined to the gas−surface interface, to probe the wetting properties of the organic surface, and to study the products that form due to reactions with atmospheric radicals and oxidants. The organic monolayers have been characterized by various surface sensitive techniques such as contact angle measurements, infrared spectroscopy (FTIR), X-ray photoelectron spectroscopy (XPS),† and laser induced fluorescence.

There are a number of recent studies using organic monolayers to understand the chemistry of organic aerosols. Organic monolayers deposited on a glass substrate have been used to probe reactive processes on surfaces of organic particles.[78,79,83,84] Organic layers at the air−water interface were also employed for studying ozone reactions[85] and for studying the partition of organic species to the surface of droplets and aqueous particles.[67] The effects of organic monolayers on mass transfer from the gas phase to the aerosol phase were also studied.[86] These proxies were used for determination of reactive uptake coefficients for purely surface reactions,[79,83,84] for understanding chemical mechanisms at the surface,[78,83] for identification of volatile and nonvolatile products from surface reactions,[78,79,83,85] for understanding the dynamics of the surface chemical reactions,[85] and for studying the effect of structure and chemistry on the ability of organic surfaces to absorb water.[72,87] The organic monolayers proxies are studied using different experimental setups, among them flowtube kinetic experiments, FTIR surface studies, experiments using molecularly controlled semiconductor resistor (MOCSER)† and quartz crystal microbalances (QCM)†, and experiments using monolayers deposited on a Langmuir trough.[72,78,79,83−85,87]

2.2. Organic Liquids and Solid Films

Organic liquids and frozen films were used in kinetic and mechanistic studies,[75,79,88−91] molecular beam scattering experiments,[92−94] and absorption experiments.[69] They were the predominant proxy used in flowtube experiments[75,79,88−91] and in QCM experiments[69] for determination of reactive uptake coefficients, mass accommodation coefficients, and solubility constants. Organic liquids and films were used also for characterization of volatile and nonvolatile products following reactions and for elucidating chemical mechanisms. Although the surface properties of liquid organic films are not easily characterized, the films enable studies that invoke a higher diversity of chemical compositions compared with the organic monolayers and therefore can mimic more closely surfaces of real aerosols, especially urban aerosols that have been shown to be liquid-like[52] and to behave similarly to octanol.[53,54,95] Organic liquids are usually used in flowtube experiments because they can easily coat the walls. Frozen organic liquids are used as a proxy for surface-only reactions.[79,90,91] The surface in these cases is not as well-defined as that of a monolayer, both in terms of smoothness and in terms of order. For studying chemical mechanisms, the organic liquids are analyzed following reactions with atmospheric radicals and oxidants and information about liquid-phase products that form during the gas−liquid interactions obtained.[90]

2.3. Liquid Droplets

Large aqueous droplets (70−300 μm diameter) have long been used to study the reactive and nonreactive uptake of trace gases employing the well-established droplet train flow tube apparatus.[68,96,97] In this technique, the depletion of a trace gas is monitored as a function of exposure to a train of falling droplets. From measurements of the uptake as a function of droplet size, the mass accommodation coefficient α can be derived. Recently, this technique has been extended to the measurements of the mass accommodation coefficients and solubility constants of representative organic and inorganic trace gases in liquid organic droplets.[98−100] Two organic liquids were studied. Octanol, a water-insoluble solvent, is considered to have properties closest to those of urban organic aerosols.[52,54,55] The other liquid is ethylene glycol, which has two OH groups and is completely miscible in water. Solutions with varying mole fractions of water were used for these experiments in order to probe the effects of relative humidity (RH) on the uptake processes. Solubility constants were derived using this experimental technique in cases where the uptake is limited by solubility. This method enables uptake experiments to be conducted at varying temperatures and thermodynamic properties to be derived for the uptake process.

2.4. Aerosols (Flow Experiments)

Aerosol flow tube experiments were employed to study the reactive uptake of ozone by liquid oleic acid aerosols[101,102] and by reaction with benzo[*a*]pyrene

(BaP) deposited on spark soot aerosols.[76] New experimental avenues became feasible following the recent development of aerosol mass spectrometers capable of providing quantitative size and chemical information about aerosols in a flow tube.[66,70,71] The aerosol experiments employ model aerosols ranging in size from the submicron[76,101] to aerosols of 5 μm in diameter.[102] These model aerosols still have simplified chemical compositions compared with the ambient environmental matrix. However, these systems add another dimension of complexity compared with the previous model systems because effects of the finite aerosol size on the reactive transformations can be probed. Therefore, these experiments are an advancement toward probing the chemistry in a well-defined environment that is closer to particles in the atmosphere. Of course, the model aerosol can be further manipulated by deposition of different layers to obtain more realistic aerosols. In addition to the uptake of a single reactant, the effects on the reactivity of RH and competitive adsorption on the reactivity have been studied in these experiments.[76]

In experiments with organic monolayers and liquids, the uptake coefficients were determined by following the disappearance of the reactant from the gas phase as a function of interaction time with the organic substrate. In the aerosol flowtube experiments, however, the reactive uptake coefficients are determined by following the disappearance of the reactive aerosol-phase component.[76,101,102] The method can also provide, in principle, information about the formation of aerosol-phase products. However, this has been implemented only to a limited extent in these experiments.[101,102]

Several studies used organic aerosols or coated inorganic aerosols to study the effect of the organic material on aerosols' ability to nucleate cloud droplets and to activate to cloud droplets under high relative humidity. These flow experiments used differential mobility analyzers (DMA)† for size selection, and thermal gradient diffusion chambers and cloud condensation nuclei counters to study the response of the particles to varying humidities[103−106] and to supersaturation† conditions pertinent to conditions in clouds.

2.5. Aerosols (Chamber Experiments)

Parameters such as reactive uptake coefficients and rate coefficients for surface reactions were determined in aerosol chambers where the organic component has been used to coat an inorganic core.[48,77,107,108] Two different approaches were used. In one approach, selected organic compounds (pesticides) adsorbed to particles, creating less than a monolayer coating, were used. Rate coefficients for surface reactions were determined by monitoring the disappearance rate of the adsorbed organic from the aerosol phase by reaction with the OH radical.[48,77,107] The other approach[109,110] used *in-situ* reaction of ozone with α-pinene to form a coating made of the reaction products on ammonium bisulfate particles. The coating thickness was varied by changing the ozone and α-pinene concentrations in the chamber. The chemical composition of the coating in this case is less defined but is expected to mimic the more realistic composition of such coatings that may be found on real atmospheric particles.

3. Laboratory Studies

3.1. Uptake of Water by Organic Surfaces: Effect of Structure and Oxidation State

Discoveries of organic layers encapsulating inorganic cores[35,38,46] and on the surfaces of cloud droplets[19] suggested that organic layers and surfaces may play an important role in determining the physicochemical properties of atmospheric particles. A key property of aerosols in general, and of organic aerosols in particular, is water uptake, as it affects both the growth of particles in response to ambient humidity as well as the uptake of organic and inorganic species, a key process for aerosol growth and chemistry. Some of the most hydrophobic organic surfaces are self-assembled monolayers† (SAM), which are characterized by a close-packing, solid-like structure. SAM have been adopted as a surrogate for organic surfaces because they allow one to follow reactive and nonreactive processes in a well-defined manner.

Rudich and co-workers[72,87] determined that water adsorbs to hydrophobic surfaces using two complementary techniques, molecular controlled semiconductor resistor (MOCSER)[111] and QCM covered by SAM. It was found that water adsorption depends on the RH and is reversible. The amount of adsorbed water followed a Langmuir isotherm and increased with surface corrugation. This was verified by the correlation between the Langmuir equilibrium constants and contact angle measurements.[72,87] The experiments, as well as molecular dynamics simulations of water adsorption on hydrophobic organic surfaces, suggest that water adsorption onto a hydrophobic organic surface proceeds via formation of small water clusters which originate on irregularities on the organic surface. The irregularities provide "nucleation" centers to which water molecules first absorb. The initial adsorption occurs at imperfections which are relatively far apart, and therefore the adsorption of water molecules on one site is independent of other sites. Due to the hydrophobicity of SAM and the strong water−water interactions, the adsorbed water can form surface-bound microdroplets. These droplets do not cover the whole surface area, as is evident in coadsorption experiments of O_2 and water.[87] Figure 1 shows the result of molecular dynamics simulations of water adsorption onto hydrophobic surfaces. Two hundred water molecules, randomly deposited on a hydrophobic smooth (only C_{18} chains) surface, quickly form a droplet on the surface in order to minimize the hydrophobic interactions and to maximize the water−water interactions.[87] When the same experiment is repeated on a rough surface (mixture of C_{18} and C_{22} chains), the water wets the surface, decreasing the water−water interactions. The rough surface is covered more by the water than the smooth one.

That the morphology of hydrophobic surfaces determines the amount of water bound to surfaces is a

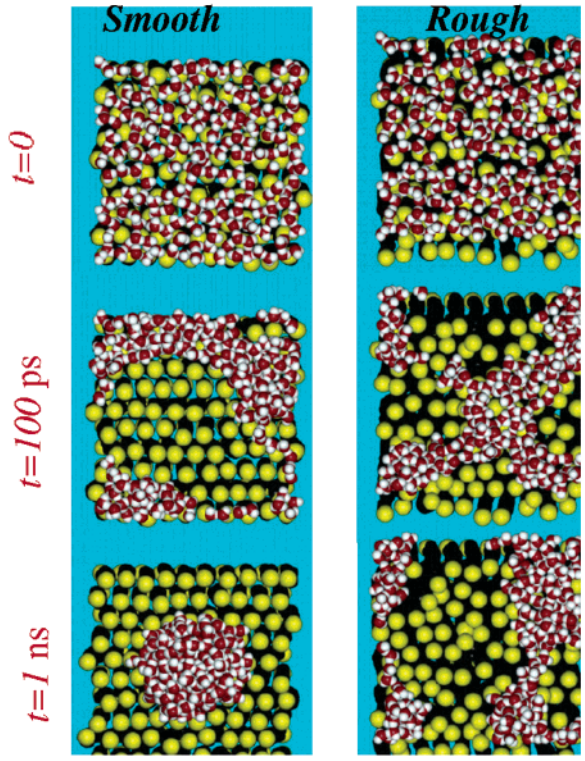

Figure 1. Molecular dynamics simulation of water in the proximity of a hydrophobic surface. The simulation initiates with 200 water molecules on a rough and smooth surface. It can be seen that while in a smooth surface (left panel) water molecules (red and white) form a droplet on the surface (yellow), they clearly wet the rough surface (right panel). Reprinted with permission from ref 87. Copyright 2000 American Chemical Society.

general phenomenon, confined not only to organic surfaces. The same process was observed for some inorganic systems. Adsorption of water on the surface of salts and mica is greatly enhanced by surface defects and atomic steps,[112−115] and corrosion of aluminum by sulfuric acid also proceeds via formation of surface defects.[116] Surface morphology also determines the structure of ice forming on hydrophobic organic surfaces.[117]

Recently Demou et al.[69] used a microbalance (QCM) to measure the uptake of water by thin ($\leq 1\ \mu$m) films of organic compounds that add chemical complexity not available with the monolayer studies. These films are composed of organic compounds possessing different degrees of oxidation: dodecane, 1-octanol, octanoic acid, 1,5 pentanediol, and malonic acid. All compounds studied displayed some sorption† of water (Figure 2). It was found that the higher the oxidation state of the organics in the film, the greater is the amount of water sorbed. For example, for a given relative humidity, the amount of water sorbed by the film increases in the order 1-octanol < octanic acid < 1,5 pentanediol.[69] The observed uptake by the hydrophobic dodecane was probably due to adsorption at surface irregularities, in accordance with the SAM results.[72,87] In the other less hydrophobic compounds, water dissolved into the film. The measured absorption isotherms were compared to the absorption predicted by the absorptive partitioning model of Pankow[118,119] using UNIFAC† calculations of activity coefficients. The model dramatically underpredicts adsorptive uptake (like that of hydrophobic films). It slightly overpredicts uptake at low relative humidities and slightly underpredicts the absorption by the oxidized organic films.[69]

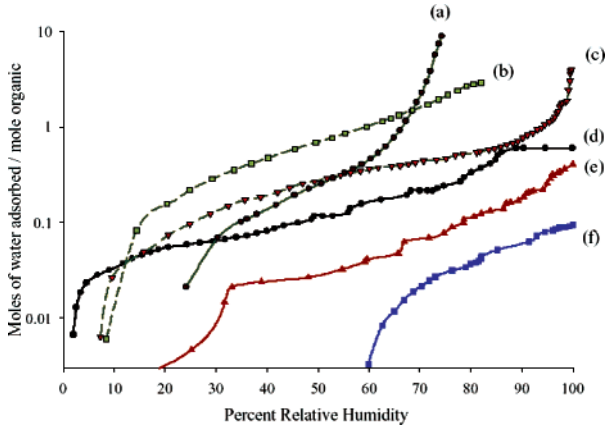

Figure 2. Absorption isotherms of water onto different organic compounds as a function of relative humidity:[69] (a) malonic acid, (b) 1,5 pentanediol, (c) 1,8 octanediol, (d) octanoic acid, (e) 1-octanol, and (f) dodecane.

The results of Demou et al.[69] distinguish between three distinct patterns of water uptake behavior by organic films. Water-soluble large organic compounds behave in a similar manner as inorganic salts; they show deliquescence†-like behavior, and exhibit hysteresis upon decrease of the relative humidity. Organic compounds which are liquids at room temperature and have limited solubility in water display a smooth water uptake with increasing RH and follow almost the same (but reverse) behavior upon drying. Very hydrophobic compounds show much reduced water uptake, probably adsorptive in nature. This classification and the observed trends can be used for estimating the uptake behavior of aerosols and model systems. As will be shown later, these results agree with nonreactive uptake measurements of organic and inorganic trace gases by organic droplets[98−100] with reactive uptake experiments in chamber experiment[108,109] and with aerosol activation experiments.[103]

The experiments with monolayers and films suggest that aerosols with hydrophobic films will respond to changes in RH and that adsorption of water will affect their chemistry and dictate their effects on visibility and the climate. It is likely that the atmosphere does not contain purely hydrophobic aerosols, and therefore the results of Demou et al.[69] can be considered to be rough guidelines for predicting the behavior of real atmospheric aerosols. Urban aerosols have been shown to behave similarly to octanol and show limited water uptake. Keeping in mind the model of water uptake by Rudich et al.,[87] some valid questions are the following: what is the possible role of surface microdroplets in determining the optical and chemical properties of organic aerosols, and can concepts from liquid-phase chemistry, such as acid−base equilibrium, and full solvation be applied to such microdroplets?

Abbatt and co-workers measured the activation† of organic acid aerosols at supersaturation†.[103] They

found that soluble organic compounds (such as oxalic, malonic, and glutaric acids) are fully activated to cloud droplets and that their behavior is well modeled by a simplified Köhler† theory, assuming that the droplet has the same surface tension as that of water.[103] Partially soluble organic compounds (such as adipic and succinic acids) are well modeled using full Köhler theory provided that partial solubility and composition-dependent surface tensions are fully incorporated.[103] Highly insoluble organic species do not activate. However, reactive organic species can be activated by oxidation processes, such as reaction with ozone that leads to production of soluble products such as azelaic acid[90,101] (see section 3.5.3.).

The observations of Abbatt and co-workers are consistent with the experiments of Cruz et al.,[104−106] who studied the cloud condensation nuclei (CCN)† activity of glutaric acid, adipic acid, and dioctyl phthalate (DOP) aerosols. They produced a nearly monodisperse distribution of submicron particles and compared the total CCN concentrations to the total number concentrations. The measurements were performed using a tandem differential mobility analyzer (DMA)† in combination with a cloud condensation nuclei counter at supersaturations of 0.30% and 1.0%. The results indicate that the more hydrophilic adipic acid and glutaric acid aerosols were CCN at both supersaturations and that their behavior is in fair agreement with Köhler theory. Hydrophobic DOP aerosols, however, with diameters up to 0.15 μm did not activate, even at a supersaturation as high as 1.2%.[105] The observed behavior of the different organic aerosols is in general consistent with the classification of Demou et al.[69]

3.2. Effect of Organic Layers on Mass Transfer

The organic interface between the atmosphere and an aerosol particle undergoes constant changes. One is the interaction with water described above. Another is the reactive and nonreactive uptake of organic and inorganic species. The nonreactive uptake process is particularly important because it will determine the aerosol's growth, its chemical composition, and the type of chemistry that it will undergo on the surface and in the bulk. Field measurements have found enriched amounts of hydrophobic and surface-active organics on the surface of fog droplets and water-covered aerosols.[19,120−122] The presence of films on droplets will affect mass transfer into the particle and its subsequent chemical reactivity.

The effect of organic layers on mass transfer and on equilibration times was investigated by several groups.[86,108,123,124] Cruz and Pandis[123] studied the evaporation of submicron ammonium nitrate (NH_4NO_3) aerosols coated by DOP. The layer thickness was between 10 and 15 nm. The evaporation rates for the organic-coated particles were compared to those of pure ammonium nitrate. Up to a 50% decrease in the NH_4NO_3 evaporation rate due to the presence of the DOP film was observed. The decrease in evaporation due to the DOP amounts to an effective decrease of the accommodation coefficient for NH_4NO_3, α, from $\alpha = 0.4$ (which is the value for pure NH_4NO_3) to $\alpha = 0.25$ for the DOP-coated NH_4NO_3. The decrease in evaporation rates can also be explained by a decrease in the NH_4NO_3 effective diffusivity.

Daumer et al.[86] studied the influence of thin organic films on the neutralization reaction of H_2SO_4 aerosol with gas-phase ammonia. They found that the film strongly suppresses the rate of neutralization depending on the molecular structure of the coating substance and the coating thickness. Straight-chain molecules such as n-hexadecane and n-hexadecanol strongly retarded the mass transfer to the sulfuric acid, while branched-chain molecules did not show a significant effect, probably because of their inability to form tightly packed films. Daumer et al. suggested that organic coatings composed of natural hydrocarbons and their degradation products also affect mass transfer.[86]

Shulman et al.[124] studied how the rate of water evaporation from droplets depends on the chemical properties of coatings composed of small difunctional, surface-active organics such as oxalic acid and adipic acid. These compounds are found in atmospheric aerosols.[31] Specifically Shulman et al. addressed the question of how the solubility and surface activity of these organics affects the evaporation process. Using an electrodynamic balance, the evaporation from water droplets containing ammonium sulfate, sodium dodecyl sulfate (SDS, a surfactant), oxalic (C_2), adipic (C_6), and *cis*-pinonic (C_{10}) acids was studied. All the compounds reduced the evaporation rate substantially when compared to evaporation from pure water droplets. The evaporation rates were almost equal for the different surfactants. This is despite their different surface concentrations which depend on their surface activity in the order SDS > *cis*-pinonic acid > adipic > oxalic > $(NH_4)_2SO_4$. Compounds that lead to a lower surface tension of water required lower surface concentrations to reduce the evaporation rate of water from the droplets. The results of this study imply that surface-active species would influence mass transfer at much lower concentrations than less surface-active compounds.

Folkers and Mentel[108] investigated the effect of films composed of natural hydrocarbons on mass transport to aqueous particles. In a series of chamber experiments, ammonium bisulfate aerosols coated with photochemical degradation products of α-pinene ozonolysis were used. These compounds are oxygenated hydrocarbons such as pinic acid, pinonic acid pinonaldehyde, and others. Some of them are mono- and dicarboxylic acids, and most of them contain a ketone or aldehyde group. The resulting organic film, although not well-defined chemically, is representative of the type of organic compounds expected to be found in rural environments. The effect of coating on the hydrolysis of N_2O_5 was determined by measuring the reactive uptake coefficient of N_2O_5, γ, in a smog chamber using infrared spectroscopy. For uncoated NH_4HSO_4 particles, $\gamma = (1.86/+0.43 - 0.35) \times 10^{-2}$ was measured, while for pure organic particles produced *in-situ* by ozonolysis of α-pinene, the value of γ was about $(0.045 + 0.015/-0.009) \times 10^{-2}$. This value is consistent, although slightly higher than $\gamma = 1 \times 10^{-4}$, which was determined for uptake of N_2O_5

by tridecane in a flowtube setup.[88] The uptake coefficient of N_2O_5 by organic-coated NH_4HSO_4 was determined to be $\gamma = (0.54 + 0.02/-0.012) \times 10^{-2}$ for a thick coating (1.22 ppm α-pinene + O_3) and $\gamma = 0.34 \times 10^{-3}$ for a thinner coating (11 ppb α-pinene + O_3).[110]

These results suggest that the organic surface slows the mass transfer from the gas phase into the ammonium bisulfate core. It was inferred that the coating slows the hydrolysis reaction due to a lower solubility of N_2O_5 in the organic film.[110] In other words, the organic coating deactivates the aerosol surface toward N_2O_5 hydrolysis, which is an important atmospheric removal pathway of NO_x from the atmosphere, especially in the presence of clouds.[125] A different experimental technique, such as electron microscopy, may be helpful in characterizing the extent of the coating. Values of the N_2O_5 uptake coefficient in the same range, $\gamma \approx 2.5 \times 10^{-3}$, were also measured for ambient aerosols.[108] This observation may imply that a similar type of organic coating is found on the surface of real ambient particles and that these low γ values should be used in modeling studies of N_2O_5 uptake.

While an organic coating of nonsoluble compounds significantly reduces the rate of hydrolysis, water soluble organics have a more complex effect on N_2O_5 heterogeneous loss.[108] Organic compounds that deliquesce at ambient RH do not exhibit any effect on the rate of N_2O_5 uptake by ammonium sulfate, while those that are not soluble substantially decrease the uptake. This observation is consistent with the results of Demou et al.,[69] who concluded that water-soluble organic compounds qualitatively behave like inorganic salts and show deliquescence-like behavior. In line with the chamber results, Thornton et al.[126] also measured a substantial decrease in γ for N_2O_5 on aerosols of dry malonic acid compared to aqueous malonic acid aerosols ($\gamma < 0.003$ and $\gamma \approx 0.015$ respectively). Another observation of Folkers and Mentel[108] is that the NO_3^- ions formed by hydrolysis of N_2O_5 quickly replace the dicarboxylic acids from the surface. These laboratory studies suggest that for ambient RH less than about 50%, there are probably not enough water molecules on the surface of organic aerosols to carry out the hydrolysis reaction and the uptake of N_2O_5 is substantially reduced compared with aqueous aerosols.

3.3. Solubility in the Organic Medium

The solubility of atmospheric trace species in the aerosol organic matrix will play an important role in determining the partitioning of species between the gas phase and organic aerosols. The gas-particle partition coefficient is commonly used in models to describe the distribution of semivolatile organic compounds (SOCs) between the gas and the particle phase. Following Pankow[127] it is defined as

$$K_P = \frac{F/\mathrm{TSP}}{A} \tag{3}$$

where K_P is the gas-particle partition coefficient ($m^3/\mu g$), F and A are the particle associated and gaseous concentration of the SOCs (ng/m^3), respectively, and TSP is the total suspended particulate matter concentration ($\mu g/m^3$). K_P depends on temperature, with an increased absorption as the temperature decreases.

The sorption of SOCs by aerosols can result from adsorption onto a solid surface, absorption into a liquid particle or into a liquid organic film encapsulating a particle, or a combination of both.[118,119] Gas-particle partitioning of SOCs by urban submicron aerosols that contain a significant amount of organic matter[128] is probably dominated by absorption into the liquid organic fraction of the aerosol.[52] Recently, it was recognized that *n*-octanol is a good surrogate for absorptive organic atmospheric particulate matter.[54,56,95] It was suggested that the octanol−air partition coefficient, K_{OA}, may be a useful tool for predicting the partitioning of SOCs between the gas and organic particulate phases. K_{OA} is defined as

$$K_{OA} = \frac{C_O}{C_A} \tag{4}$$

where C_O and C_A are the concentrations of the SOCs in octanol and in air, respectively. Using an absorption model[118,119] and assuming that the fraction of organic matter is 20% of the aerosol mass and that all of the aerosol organic matter is available to absorb gaseous compounds, a relationship between K_P and K_{OA} was developed:[54,95]

$$\log K_P = \log K_{OA} - 12.61 \tag{5}$$

This relationship holds for several SOCs classes, such as polychlorinated biphenyls (PCBs), polycyclic aromatic hydrocarbons (PAHs), and polychlorinated naphthalenes (PCNs).[54,56,95]

Several solubility constants for organic and inorganic species in octanol were derived using the droplet train flowtube apparatus.[99,100] This technique measures the product of the solubility constant and the liquid-phase diffusion coefficient, $H\sqrt{D_l}$, rather than the actual solubility constant. However, if the diffusion coefficient is known or estimated, the solubility constant H can be calculated. The solubility constant in octanol (H_{OA}) relates to K_{OA} by $K_{OA} = H_{OA} \times R \times T$ (R is the gas constant, T is the temperature). Using the droplet train apparatus the temperature-dependent solubility constants are obtained. The following expressions for the temperature dependence of H in octanol were derived:[99]

α-pinene: $\ln H\,(\mathrm{M/atm}) = -(6.95 \pm 1.16) + (3.80 \pm 0.31) \times 10^3/\mathrm{T}$

with $H = 475$ M atm^{-1} at 298 K

acetic acid: $\ln H\,(\mathrm{M/atm}) = -(30.30 \pm 6.90) + (10.6 \pm 1.85) \times 10^3/\mathrm{T}$

with $H = 200$ M atm^{-1} at 298 K

HCl: $\ln H\,(\mathrm{M/atm}) = -(4.50 \pm 1.10) + (3.53 \pm 0.23) \times 10^3/\mathrm{T}$

with $H = 7.5\ \mathrm{M\ atm^{-1}}$ at 298 K

HBr: $\ln H\,(\mathrm{M/atm}) = -(9.11 \pm 2.81) + (5.19 \pm 0.75) \times 10^3/\mathrm{T}$

with $H = 4 \times 10^4\ \mathrm{M\ atm^{-1}}$ at 298 K

These solubility constants imply that these substances would not substantially partition into organic aerosols in the atmosphere.

Treves et al.[73] developed a new method for the determination of K_{OA} using solid-phase microextraction (SPME)†. The method determines the solubility constant in a liquid, such as octanol, relative to another compound with a known Henry's law constant by measuring the headspace concentrations over diluted solutions. The technique was applied to the determination of temperature-dependent K_{OA} of β, γ, and δ C_3-C_5 hydroxy alkyl nitrates which are common atmospheric multifunctional organic nitrates.[129−133] The room-temperature Henry's law constants determined by SPME ranged between 2×10^4 and 3×10^5 M atm^{-1}, compared with $H = 5-200$ M atm^{-1} typically found for C_4 and C_5 alkyl nitrates.[73] The temperature dependence of the solubility constants in octanol between 275 and 306 K was determined, and values for the enthalpy of phase transfer (ΔH_O) were derived[73] (see Figure 3). The solubility constants of

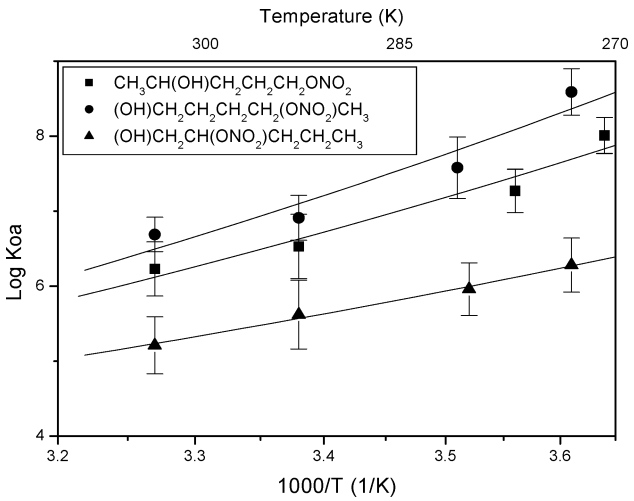

Figure 3. Plot of log K_{OA} as a function of $1/T$ for several alkylhydroxy nitrates between 275 and 306 K.[73]

these multifunctional compounds are higher in octanol than in water, and their solubility in octanol increases with the length of the hydrophobic chain and with increasing distance between the hydroxy and the nitrooxy groups.[73] These results imply that oxygenated multifunctional hydrocarbons will tend to partition more into organic aerosols than hydrophobic compounds that have comparable chain length and vapor pressure.

3.4. Nonreactive Uptake Experiments

Mmereki et al.[67] studied the partitioning of pyrene to hexanoic acid coated water surfaces using laser induced fluorescence of the surface-bound pyrene. They found higher concentrations, up to a factor of 2, of pyrene at the hexanoic-acid-coated water surface, compared with uncoated aqueous solutions. This result can be understood in terms of pyrene's affinity to partition to octanol from water. Pyrene has $K_{OW} = 5.8$ (K_{OW} is the partition equilibrium constant between water and octanol). It was previously proposed that compounds with $K_{OW} > 2$ are expected to favorably partition into surface films.[120] Even for submonolayer coating by the acid, enhancement of pyrene's surface concentration was observed. The concentration of pyrene at the interface scaled linearly with its bulk concentration until a saturation point which depended on the surface concentration of hexanoic acid.[67] This study suggests that surfaces of organic-coated aqueous droplets may contain higher concentrations of hydrophobic chemicals than uncoated particles. The surface concentration of the absorbed species may be higher than that predicted by their Henry's law solubility constant. Species absorbed by a surface organic coating may be subject to reactions with colliding atmospheric oxidants. Oxidants and radicals that form by photochemical processes inside the aqueous phase, such as OH and reactive oxygen, can also react with organic species absorbed in an organic coating. Reactive processes will be discussed in section 3.5.

The mass accommodation coefficient determines the efficiency by which molecules transfer from the gas to the aerosol phase. To determine mass accommodation coefficients pertinent to organic aerosols, uptake experiments with organic droplets using octanol and ethylene glycol droplets were conducted.[98−100] Ethylene glycol is a surrogate for photochemically processed hydrophilic organic aerosol and octanol possesses properties pertinent to urban aerosols.

The mass accommodation coefficients (α) of HCl and HBr on ethylene glycol were measured as a function of temperature and water mole fraction (0−1). At 0% relative humidity, the mass accommodation coefficient of HBr is $\alpha = 1$, independent of temperature. For HCl, α is lower, and it increases with decreasing temperature ($\alpha = 0.4 \pm 0.06$ at 303 K to $\alpha = 0.79 \pm 0.12$ at 258 K).[98] Negative temperature dependence for α has been observed also for uptake on liquid water and was successfully explained using a surface-nucleation model.[134,135] On the basis of experiments with DCl, it is concluded that the thermal mass accommodation of HCl is $S = 1$, indicating a strong interaction with the surface molecules. The higher α values for HBr compared with HCl are indicative of a stronger interaction of HBr with the organic surface. These observations are consistent with low kinetic energy molecular beam scattering experiments with glycerol; nearly all HBr molecules thermalize at glycerol surfaces, and ~100% of these molecules enter the bulk.[93,134] In contrast, only 50% of thermalized HCl molecules enter the liquid, and the rest desorb back to the gas.

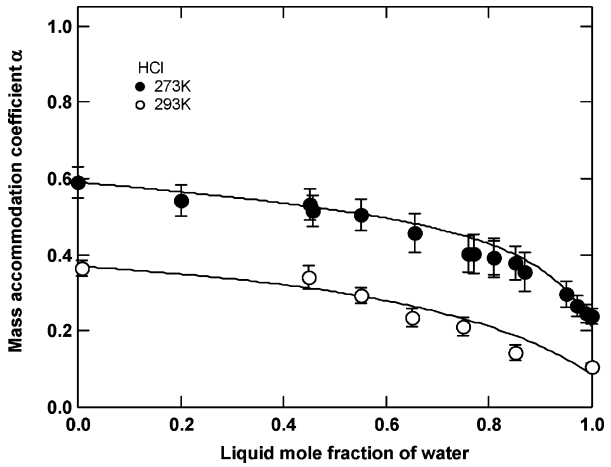

Figure 4. Mass accommodation coefficient γ for HCl on ethylene glycol−water surfaces as a function of water mole fraction from 0 to 1 at 273 K (filled symbols) and 293 K (open symbols). Solid lines are the calculations based on surface-tension parametrization. Reprinted with permission from ref 98. Copyright 2002 American Chemical Society.

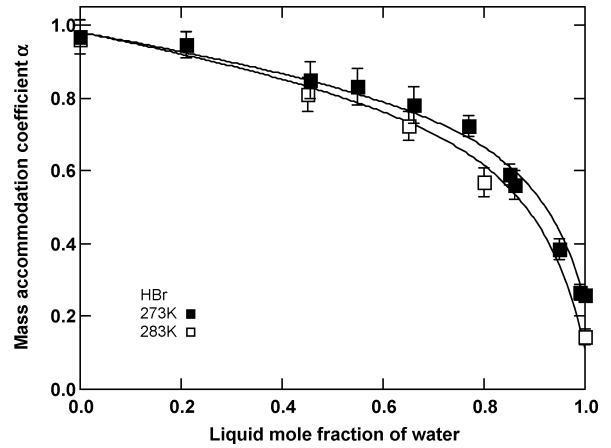

Figure 5. Mass accommodation coefficient γ for HBr on ethylene glycol−water surfaces as a function of water mole fraction from 0 to 1 at 273 K (filled symbols) and 283 K (open symbols). Solid lines are the calculations based on surface-tension parametrization. Reprinted with permission from ref 98. Copyright 2002 American Chemical Society.

The values of the uptake coefficients of HCl and HBr on ethylene glycol change smoothly as a function of water mole fraction in the droplet. At 0 mol fraction of water, the α values are those measured on pure ethylene glycol, decreasing to the measured value of α on pure water.[98] Figures 4 and 5 show the dependence of the uptake coefficient α as a function of RH for HCl and HBr at two different temperatures. The nonlinear behavior suggests that α does not change as the bulk mole fraction but is weighted by the fractional surface coverage $X(s)_{H_2O}$

$$\alpha = \alpha_{H_2O} X(s)_{H_2O} + \alpha_{EG}(1 - X(s)_{H_2O}) \qquad (6)$$

where α_{EG} is the mass accommodation coefficient on the pure liquid. Li et al.[98] suggested that the surface coverage may be proportional to the surface tension of the ethylene glycol−water mixture, i.e.

$$\sigma = \sigma_1 X(s)_{H_2O} + \sigma_2(1 - X(s)_{H_2O}) \qquad (7)$$

where σ_i is the surface tension of pure component i. This formulation and its concept are convenient since the surface tension as a function of the bulk composition of the ethylene glycol−water mixture is known.[136] Indeed, a fit of the data to this functional form is convincing,[98] suggesting that surface tension may be a determining parameter for other processes occurring on the surface of hydrophilic organic liquids and aerosols.

Zhang et al.[99,100] studied the uptake of HCl, HBr, HI, α-pinene, γ-terpinene, *p*-cymene, 2-methyl-3-hexanol, and acetic acid by droplets of octanol, a more hydrophobic organic liquid. The studies were conducted as a function of temperature and relative humidity. The mass accommodation coefficients of γ-terpinene, *p*-cymene, and 2-methyl-3-hexanol exhibit negative temperature dependence (Table 1).

Table 1. The Mass Accommodation Coefficients (α) for γ-Terpinene, *p*-Cymene, and 2-Methyl-2-hexanol on 1-Octanol at the Temperatures Shown Corresponding to Figure 6

	α		
T (K)	γ-terpinene	*p*-cymene	2-methyl-2-hexanol
265	0.124 ± 0.015	–	–
267	0.113 ± 0.014	0.201 ± 0.020	–
269	0.107 ± 0.012	0.168 ± 0.021	0.246 ± 0.028
273	0.097 ± 0.012	–	–
275	0.103 ± 0.015	0.165 ± 0.022	0.220 ± 0.027
282	0.093 ± 0.011	0.135 ± 0.014	0.162 ± 0.018
286	0.088 ± 0.011	–	–
290	0.076 ± 0.010	0.097 ± 0.016	0.112 ± 0.013

Reprinted with permission from ref 100. Copyright 2003 American Chemical Society.

Figure 6 shows how α changes with temperature for γ-terpinene, *p*-cymene, and 2-methyl-2-hexanol. For HBr and HI, α approaches unity, while α = 0.01 for HCl (at 298 K).

The α values for the uptake of the studied organics by octanol do not depend on the water mole frac-

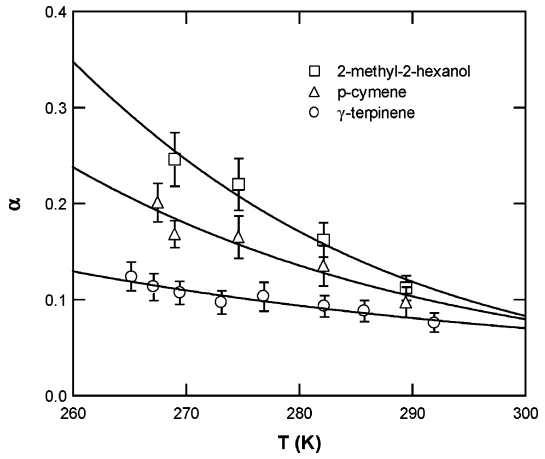

Figure 6. Mass accommodation coefficients (α) for γ-terpinene (○), *p*-cymene (△), and 2-methyl-2-hexanol (□) on 1-octanol as a function of temperature. Solid lines are obtained via eq 10 in ref 100 with ΔH_{obs} and ΔS_{obs} values listed in Table 1. Reprinted with permission from ref 100. Copyright 2003 American Chemical Society.

tion.[100] This can be understood since there is no evidence that the low water mole fraction alters the surface tension or the bulk properties of the octanol−water mixture compared with those of pure octanol. This is in contrast to addition of as little as 10^{-5} mol fraction of octanol to water, which dramatically changes the surface tension of water, probably due to segregation of the alcohol to the surface.[99] The α values of the organics suggest that the surface of octanol−water solutions consists predominantly of octanol molecules, in line with the observations for hydrophobic films.[69,87]

The behavior of α as a function of RH for the organic species can be explained using the nucleation model of Davidovits et al.[135] The model assumes a two-step process for the uptake, which involves surface adsorption followed by a competition between desorption back to the gas phase and solvation.[97,100,135] The model also postulates that there is a critical size of a cluster at a dynamic surface, that can lead to condensation and solvation.[100,134,135] Using the model, thermodynamic properties such as the parameter $\Delta G_{obs} = \Delta H_{obs} - T\Delta S_{obs}$, which is the Gibbs free energy of transition state between the gas-phase and solvated molecules, can be derived. The thermodynamic properties can be obtained directly from the temperature dependence of the α values. A linear relationship between ΔH_{obs} and ΔS_{obs} is observed for uptake by aqueous solutions and for uptake of the organic species on octanol. However, for octanol the value of the slope is different than that found for aqueous solutions.[100] Figure 7 shows the relationship

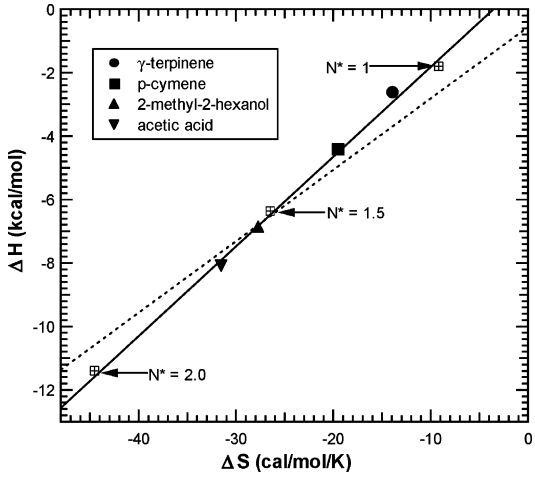

Figure 7. Experimental and calculated values of ΔH_{obs} and ΔS_{obs} for uptake on octanol. Symbols: γ-terpinene (solid circle); *p*-cymene (solid square); 2-methyl-2-hexanol (triangle); acetic acid (inverse triangle); calculations (crossed square). The dashed line in the figure is the calculated $\Delta H_{obs}-\Delta S_{obs}$ relationship for water. Reprinted with permission from ref 100. Copyright 2003 American Chemical Society.

between ΔH_{obs} and ΔS_{obs} for the uptake of the organic species on octanol (solid line) together with that obtained for uptake by water (dashed line).[100]

While no dependence of α on the RH is observed for all the organic species studied, the values of α for HCl, HBr and HI depend on the relative humidity. As RH increases, α for HBr and HI decrease, while α of HCl increases (Figure 8). At RH ≈ 50% and

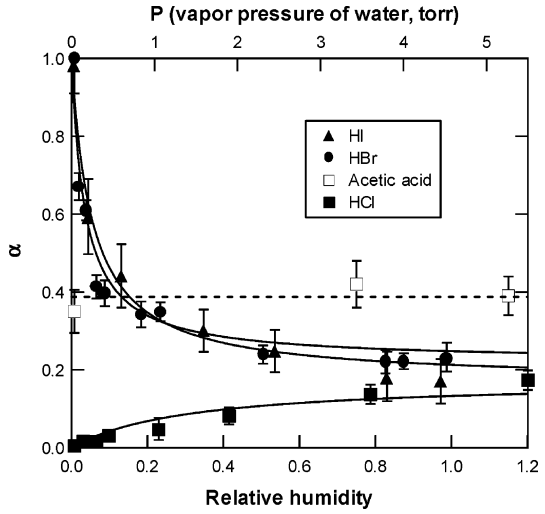

Figure 8. Mass accommodation coefficients (α) as a function of RH: HCl at 273 K (■); HBr at 273 K (●); HI at 273 K (▲); acetic acid at 266 K (□). Solid lines are the best fits via eq 7.[98]

water mole fraction < 0.2, their α values approach the values measured for uptake by pure water.

The uptake of the halides by octanol probably proceeds through the formation of a surface-bound complex

$$C_8H_{17}OH + HX \Leftrightarrow C_8H_{17}OH \cdots HX \Leftrightarrow C_8H_{17}OH_2^+X^- \quad \text{(R1)}$$

The trend in α values is compatible with the polarizability and acidity of the halides, which increase in the order HCl < HBr < HI. However, the strong dependence of α on RH for the hydrogen halides suggests that their uptake process involves interaction with water on the surface. While we know that water adsorbs to hydrophobic surfaces,[69,72,87] it is not expected to dominate the surface composition and properties. A three-step Langmuir−Hinshelwood kinetic model that explains the observed behavior was proposed by Zhang et al.[99] This mechanism involves competition between three channels: (1) fast desorption from the surface, (2) solvation into the bulk liquid, and (3) formation of a $HX-H_2O$ surface complex, which can undergo further dissociation or solvation. The model has been used to estimate the magnitude of various basic physicochemical parameters such as the rate constants for desorption, but since most of these parameters are not yet available, it is difficult to assess whether this mechanism explains all the observations. It is noted, however, that the rate coefficients derived for the surface reaction of HCl with water are substantially higher than rate coefficients for surface reactions that were derived for other reactive systems.[75,76] For the purpose of this review, though, it is important to note that the Langmuir−Hinshelwood formulation generally applies to other reactions on surfaces of atmospheric particles (see section 4).[75,76,137−139]

3.5. Reactive Uptake Experiments

Surface-adsorbed organic species may react with atmospheric oxidants and radicals colliding with the

surface.[76,79,83−85,89−91] Surface reactions can determine the atmospheric fate and lifetime of organic matter adsorbed to the surface of aerosols. Surface-adsorbed PAH and pesticides, as well as other pollutants, will react with OH, ozone, NO_3, and NO_2.[75−77,107] The reaction with NO_2 may be of special interest since the nitration products may absorb visible light, and therefore change the optical properties of the particles.[140] Reactions of the surface-adsorbed species may lead to release of photochemically active species such as HONO and aldehydes.[78,141] Kinetics experiments conducted to quantify the reactive uptake of atmospheric oxidants such as OH and NO_3, ozone and NO_2 by a suite of proxies for organic aerosols are discussed in the following sections.

3.5.1. Uptake of Ozone: Kinetics Studies Using Organic Liquids and Surfaces

The kinetics of ozone uptake by proxies for organic aerosols is the most studied reactive process so far. Due to the wealth of information, we will divide the discussion to kinetic experiments and to studies devoted to products identification.

Using a low-pressure flowtube coupled to a chemical ionization mass spectrometer (CIMS), de Gouw and Lovejoy[89] found that ozone ([O_3] between 1×10^8 and 5×10^9 cm^{-3}) reacts efficiently with organic liquids containing double bonds (1-tridecene, α-pinene, toluene, methacrolein and canola oil). Much smaller uptake of ozone by an aldehyde (tridecanal), a ketone (2-tridecanone), an alkane (tridecane), an alcohol (1-tridecanol), and an acid (tridecanoic acid) was measured. The reactive uptake coefficients showed only weak dependence on temperature, except for a reversible large drop in γ observed upon freezing of tridecene and canola oil. No effect on γ upon freezing was observed for α-pinene. The reactive uptake coefficient was higher for smaller molecules, probably due to the higher concentrations of reactive sites.[89]

De Gouw and Lovejoy calculated that reactions of ozone with aerosols containing unsaturated organic species may lead to an ozone loss rate of 1.1×10^{-7} s^{-1}, corresponding to an atmospheric lifetime of approximately 100 days,[89] which is comparable to the 150-day photochemical lifetime calculated for ozone in mid-latitudes in the winter.[142] De Gouw and Lovejoy therefore suggested that depending on aerosol composition and number density, loss on organic particles may be a significant pathway for ozone loss in the troposphere and a source for gas-phase and aerosol-phase species. Currently no available field or model studies suggest an intense heterogeneous loss of ozone on organic aerosols, but it may be evident in environments with low NO and high aerosol loading. Some modeling studies, however, suggest that ozone loss on other aerosol types, such as dust, may be important.

In another set of experiments, Moise and Rudich[79] measured the uptake coefficients of ozone (10^8−10^9 cm^{-3}) due to reaction of ozone with SAM surfaces and liquids of terminal alkenes. They measured negligibly small uptake coefficients on surfaces and liquids of alkanes and much higher uptake by surfaces and liquids of alkenes. In addition, the uptake coefficients of ozone due to reaction with liquid alkenes were about an order of magnitude higher than those measured on frozen alkenes or on SAM surfaces (see Figure 9 and Table 2). The sharp decrease in γ due to freezing was reversible, as was also observed by de Gouw and Lovejoy.[89] The uptake by an alkene surface diminished with time. This was attributed to depletion of the double bonds on the surface by the reaction with ozone.[79]

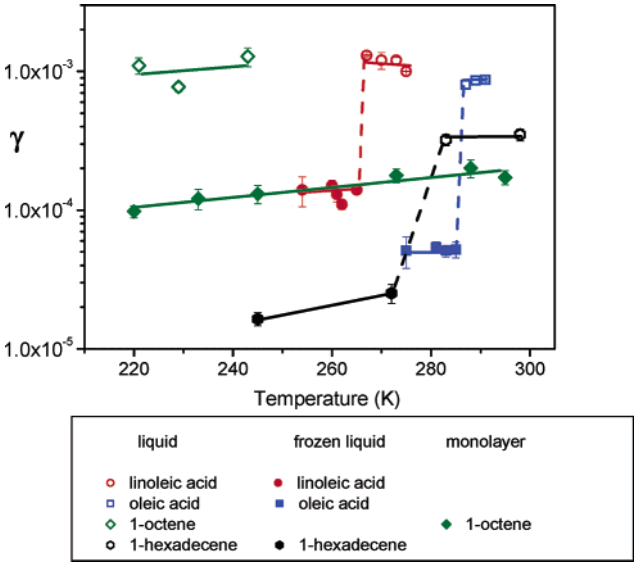

Figure 9. The reactive uptake coefficients of ozone for liquids, frozen liquids, and monolayers of aliphatic alkenes and unsaturated acids.[79,90] Reprinted with permission from ref 90. Copyright 2002 American Chemical Society.

It was suggested that the uptake by the liquid organics is higher than that by a surface, probably due to solubility of ozone followed by reaction in the bulk of the organic liquid. This suggestion was supported by the negligibly small uptake observed

Table 2. A Comparison between the Values of γ, the Reactive Uptake Probability, of O_3 and NO_3 for Saturated and Unsaturated Aliphatic Organic Monolayers, Liquids, and Frozen Liquids of Identical or Near-Identical Chain Length Which Were Measured at Similar Temperatures[a]

		liquid γ	frozen liquid γ
O_3	1-octene[79]	$(1.1 \pm 0.2) \times 10^{-3}$	
	1-tridecene[79]	$(5.5 \pm 0.8) \times 10^{-4}$	$(7.7 \pm 0.9) \times 10^{-5}$
	1-hexadecane[79]	$(2.0 \pm 0.6) \times 10^{-5}$	
	1-hexadecene[79]	$(3.2 \pm 0.2) \times 10^{-4}$	$(6.4 \pm 1.0) \times 10^{-6}$
	oleic acid[90]	$(8.3 \pm 0.2) \times 10^{-4}$	$(5.2 \pm 0.1) \times 10^{-5}$
	oleic acid[103]	$(7.4 \pm 1.) \times 10^{-4}$	
	oleic acid[101] (aerosol)	$(1.6 \pm 0.2) \times 10^{-3}$	
	oleic acid[102] (aerosol)	$(5.8-9.8) \times 10^{-3}$	
	linoleic acid[90]	$(1.2 \pm 0.2) \times 10^{-3}$	$(1.4 \pm 0.1) \times 10^{-4}$
	n-hexadecane	$(2.6 \pm 0.8) \times 10^{-3}$	$(3.8 \pm 1.0) \times 10^{-4}$
	canola oil[89]	7×10^{-4}	2×10^{-5}
NO_3[91]	1-hexadecene	$(3.8 \pm 1.0) \times 10^{-3}$	$(2.6 \pm 0.8) \times 10^{-3}$
	n-octanoic acid	$(2.1 \pm 0.3) \times 10^{-3}$	$(4.0 \pm 0.8) \times 10^{-4}$
	1-octadecene	$(1.6 \pm 0.3) \times 10^{-3}$	$(1.4 \pm 0.1) \times 10^{-3}$
	1-octanol	$(7.1 \pm 1.6) \times 10^{-3}$	$(4.1 \pm 1.0) \times 10^{-3}$
	7-tetradecene	$(5.8 \pm 2.) \times 10^{-3}$	$(5.2 \pm 2.0) \times 10^{-3}$
	linoleic acid	$(1.5 \pm 0.2) \times 10^{-2}$	$(1.1 \pm 0.3) \times 10^{-2}$

[a] C_8, C_{16}, and C_{18} refer to the number of carbon atoms in the aliphatic chain.

on liquid alkanes, which is a nonreactive process.[79,89] In follow-up experiments, Moise and Rudich also measured the uptake of ozone by oleic (9-octadecenoic) and linoleic acids (18 carbon carboxylic acids with one or two double bonds, respectively).[90] Oleic acid is a fatty acid found in urban aerosols[143] and is a proxy for compounds that are expected to be found on the surfaces of aerosols in the marine boundary layer.[35] The reactive uptake coefficients, γ, were determined to be $\gamma = (8.3 \pm 0.2) \times 10^{-4}$ and $\gamma = (1.2 \pm 0.2) \times 10^{-3}$ for liquid oleic and linoleic acid, respectively. A sharp reversible decrease of γ was observed upon freezing; $\gamma = (5.2 \pm 0.1) \times 10^{-5}$ and $\gamma = (1.4 \pm 0.1) \times 10^{-4}$ for frozen oleic and linoleic acid, respectively. As can be expected, the uptake by linoleic acid is higher than that by oleic acid due to the higher concentration of reactive sites (double bonds). The uptake by the liquid is proportional to the square root of the concentration of double bonds, as can be expected for reacto-diffusive processes.[68] No temperature dependence was observed for the liquid or surface uptake in the probed temperature range except for the sharp decrease due to freezing. A similar uptake coefficient ($\gamma = (7.4 \pm 1.0) \times 10^{-4}$) was measured for ozone uptake on oleic acid liquids in a different low-pressure flowtube. De Gouw and Lovejoy[89] measured the uptake of ozone by canola oil, a mixture of mostly oleic, linoleic, and linolenic acids, in flow tube experiments and determined a γ value of $\sim 7 \times 10^{-4}$ for the liquid and $\sim 2 \times 10^{-5}$ for the frozen liquid. In general, these values are in agreement with the measurements of Moise and Rudich.[90]

3.5.2. Ozone-Surface Reaction Mechanism

The kinetics experiments with SAM and organic liquids enabled differentiation between the uptake of ozone which is confined to the first layer of an organic surface and the reaction that occurs in the bulk of the liquid. The use of proxies allowed the elucidation of the reaction mechanism and the characterization of the surface-bound products, the bulk products, or those reaction products that are released to the gas phase. Using infrared spectroscopy of SAM on glass slides, Moise and Rudich[79] showed that the reaction of ozone proceeds exclusively by reaction with the double bonds. The adsorption lines of the remaining organic film were broader and shifted compared with the fresh surface—an indication of surface disorder induced by the reaction. No changes in the IR spectra were observed in surfaces of alkanes exposed to ozone.[79] The contact angle of water with the surface dropped by about 20° following the reaction with alkene-containing surfaces, indicating that following ozonolysis, the organic hydrophobic surface became more hydrophilic and corrugated.[78] Fully reacted surfaces exhibit no IR absorption due to double bonds. Absorption due to the alkyl backbone remains however, and the integrated intensity did not change within experimental uncertainties. In addition, organic monolayers of the C_8 alkane did not exhibit any ozone uptake.[79] Alkene surfaces became nonreactive toward ozone after all of the double bonds were consumed.

Following exposure of the monolayers to ozone, the presence of carbonyls and carboxylic acids was observed on the surface using attenuated total reflection (ATR) IR spectroscopy.[78] Products released to the gas phase were identified using IR spectroscopy. These include CH_2O, HCOOH, CO, and CO_2. Under dry conditions, the yield for production of gas-phase formaldehyde was 0.5 ± 0.1 for organic monolayers of allyltrichlorosilane ($C_3^=$, three carbon chain with a terminal double bond) and octenyltrichlorosilane ($C_8^=$), similar to the yields observed for gas-phase ozonolysis of terminal alkenes. The CH_2O yield decreased with increasing RH. A low yield (<5%) of formic acid was also observed, but only in ozonolysis of $C_3^=$ surfaces and only at low pressure. The absence of formic acid in higher-pressure experiments may be attributed either to efficient stabilization of the excited Criegee intermediate (CI), to a decrease in formic acid's already low formation yield, or to removal by efficient pressure-dependent reactions of formic acid with Criegee radicals either on the surface or in the gas.[144] No formation of OH from the surface reaction was detected, in line with the observations from gas-phase experiments in which the OH yield from alkene-ozone reactions was shown to decrease with hydrocarbon size.[145,146] On the basis of these observations, it was suggested that the reaction of ozone on the surface proceeds similarly to that in the gas phase.[78]

The reaction of ozone with unsaturated organics at the air−water interface was also studied by Wadia et al.[85] at room temperature. The reaction with a surface of the unsaturated phospholipid 1-oleoyl-2-palmitoyl-*sn*-glycero-3-phosphocholine (OPPC) and of the fully saturated phospholipid dipalmitoyl-L-α-phosphatidylcholine (DPPC) were studied by monitoring the formation of gas-phase products. The reaction in these experiments occurs in the middle of the hydrocarbon backbone. The experiments were performed by varying the surface area per molecule, corresponding to different degrees of compression of the monolayer, from a loose, gaslike configuration of the surface molecules to a compressed, ordered, and solidlike configuration. The reaction of the unsaturated compound (OPPC) produced nonanal which was detected in the gas phase by mass spectrometry. The nonanal yield per ozone reaction was determined to be (52 ± 1)%, taking into account the solubility of nonanal in the organic layer. The observed yield was invariant of the extent of surface compression. The production of nonanal decreased in time following the consumption of the reactive sites, in accordance with similar observations of surface reactions.[75,79] On the basis of kinetic calculations, Wadia et al.[85] conclude that the reaction with the surface alkenes occurs faster than is estimated based on the gas-phase reactivity of ozone.

The experimental observations of Wadia et al.[85] were corroborated by using molecular dynamic simulations. The simulations predicted that the probability of ozone encountering the double bond is independent of the extent of packing, because the density of the double bond, centered in the middle of the molecule, is not a strong function of the packing.[85] The simulations also showed that ozone is trapped between the chains for a longer time than would be

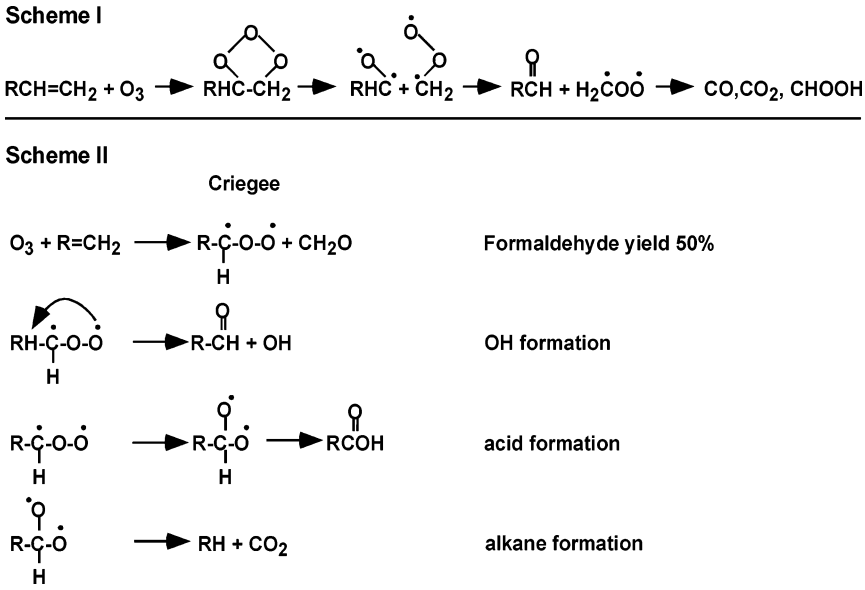

Figure 10. Proposed reaction mechanism for ozone surface reaction with terminal alkenes. Reprinted with permission from ref 78. Copyright 2001 American Geophysical Union.

predicted by a simple gas kinetic calculation, thereby enhancing the probability for reaction.[85] Finally, no evidence for OH production was observed, in agreement with the observations of Thomas et al. from experiments with terminal alkenes.[78]

A proposed gas−surface reaction mechanism is described in analogy to gas-phase reactions[144,145,147−149] and is shown in Figure 10. It proceeds by the initial insertion of the ozone to the double bond forming a primary ozonide on the surface, which can rearrange to form a secondary ozonide (similar to liquids), stabilize, or decompose. In the first decomposition pathway (Scheme 1, Figure 10), a Criegee intermediate[149] (CI) is released to the gas phase while an aldehyde forms on the surface. For reactions with terminal alkenes, the released CI can undergo a series of reactions yielding products such as CH_2O, HCOOH, CO, CO_2 and water, which were observed in the experiment.[78] For reactions of alkenes with internal double bonds, larger aldehydes form, such as nonanal.

In a second reaction channel, the surface-bound primary ozonide decomposes (Scheme 2, Figure 10) by releasing an aldehyde accompanied by formation of a surface-bound CI. This channel, based on the CH_2O and nonanal yield measurements, amounts to $\sim 0.5 \pm 0.1$ of the reaction. This yield is in agreement with the observed yield in gas-phase ozonolysis of straight chain alkenes in which formaldehyde is produced through the initial decomposition of the primary ozonide.[144,145] The counterpart of the released CH_2O is probably a surface-bound CI that can decompose via several conceivable pathways:

(a) Formation of carbonyls and/or carboxylic acids. The absorption features observed in the IR spectra are typical for carbonyls and carboxylic acids. These functional groups may form following a rearrangement of the CI and reactions with gas-phase oxygen.

(b) Formation of OH. However, no evidence for OH production was observed.

(c) Formation of methyl groups and release of CO_2 to the gas phase. This channel has been observed in the gas phase[150] and in the surface experiments.[78]

In the atmosphere, the alkoxy radicals formed on the surface can further react with nitrogen oxides or peroxy radicals (such as HO_2) present in the atmosphere. These secondary reaction channels have not been studies systematically.

To summarize: ozone-surface reactions release gas-phase species such as CO, CO_2, and aldehydes. Some of these products are photolabile (such as aldehydes). The formation of carbonyls and aldehydes on the surface suggests that in addition to the changes in surface hygroscopicity, surfaces of organic aerosols can also become more optically active.

3.5.3. Ozone-Liquid Reaction Mechanism

Volatile products from the ozone reaction with oleic and linoleic acids were monitored using electron impact mass spectrometry and with ozone concentrations in the range of $5 \times 10^{13}-5 \times 10^{14}$ molecules cm^{-3}.[90] The volatile product from the ozone and oleic acid reaction is 1-nonanal, produced with about 40% yield. A similar yield for nonanal production (0.50 ± 0.10) was measured by Abbatt and co-workers. This is a lower limit for the nonanal yield, as some of the produced nonanal may dissolve in the organic matrix. The yield increased when ozone reacted with frozen oleic acid, presumably because all of the produced nonanal evaporated to the gas phase. In liquid reactions some of the nonanal dissolves in the liquid. The mass spectrum observed following the reaction of ozone with linoleic acid is more complex and depicts a number of volatile products assigned as 2-nonenal, 4-nonenal, and 1-hexanal. The nonanal yield is comparable with that measured by Wadia et al.[85]

In the liquid phase, azelaic acid was identified as the major product of the ozone and oleic acid reaction, using ion chromatography. Nonanoic acid was also

identified as a product of the reaction of ozone with linoleic acid.[90,103] It is also possible that the 9-ozononanoic acid is a product.

On the basis of these observations the reaction mechanism of ozone with liquid alkenes can be described. In the gas phase, the reaction proceeds via the insertion of ozone into the unsaturated bond to form a primary ozonide that dissociates. An aldehyde and a Criegee intermediate (CI) are the products. In the liquid phase, the excess energy in the CI can be redistributed and solvent cage effects increase the probability that the CI will recombine with the carbonyl compound to form a stable secondary ozonide as the main reaction product.[149,150] In the gas phase, the two fragments separate rapidly and the Criegee biradical, which contains excess energy, can stabilize or decompose in a number of channels, leading to different products such as RCO, RCOOH, CO_2, CO, H_2O, and OH.[151]

The products (nonanal, hexanal, azelaic acid, nonanoic acid) observed in the liquid experiments can form via the pathways shown in Figure 11. 1-Nonanal and nonenal form via the cleavage of a primary ozonide formed at the C9 position (Figure 11a and 11b-1) and are released to the gas phase. For the linoleic acid (2 double bonds), the un-reacted unsaturated bond at the now C3 position migrates to either the C2 or C4 position. The migration to the C2 position is favorable since the conjugation between the carbon−carbon double bond and the carbon−oxygen double bond adds stability to the molecule.[152] 1-Hexanal and nonenal are produced from the primary ozonide formed at the C12 position (Figure 11b-2). These products were monitored in the gas phase.[90]

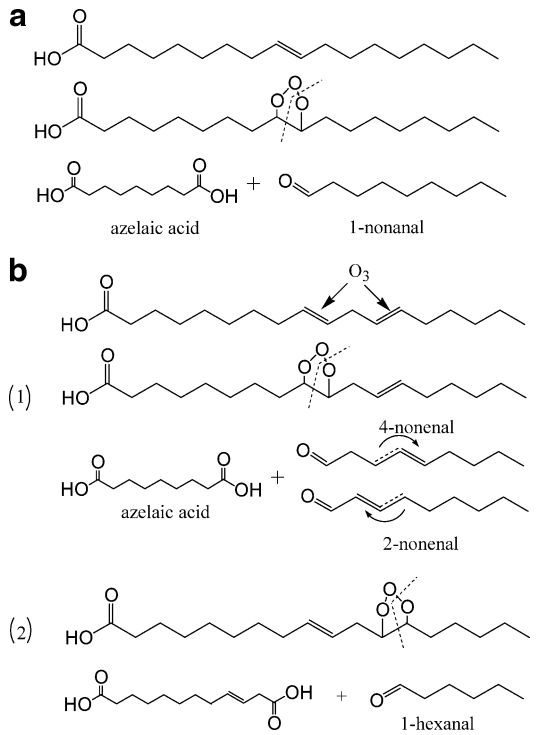

Figure 11. Proposed reaction schemes for formation of observed products by Moise and Rudich.[90] Azelaic acid was identified in the in aerosols from the Eastern Mediterranean.[154] Nonanoic acid and 9-oxononanoic acid are the other possible products, which were detected in field measurements[178,179] and assumed by Smith et al.[102] (a) Formation of 1-nonanal from the ozone reaction with oleic acid. Azelaic acid remains in the bulk liquid. (b) Formation of (1) 2-nonenal and 4-nonenal and (2) 1-hexanal from the ozone reaction with linoleic acid. Reprinted with permission from ref 90. Copyright 2002 American Chemical Society.

In the liquid phase, rearrangement of the Criegee biradical following stabilization can lead to the formation of dicarboxylic acids such as azelaic acid which was detected following reaction with oleic acid. The formed acids remain in the liquid phase due to their low volatility (Figure 11a,b-1).[90] The counterpart product for the nonanal is nonanoic acid, which remains in the liquid phase and was detected. 9-Oxononanoic acid was not identified due to lack of standards.

Azelaic acid, one of the complementary organics to the 1-nonanal and nonenal volatile products, remains in the aerosol phase due to its low volatility. Dicarboxylic acids are recognized as ubiquitous organic aerosol constituents.[153,154] Although diacids with higher carbon numbers are generally less abundant than the smaller acids, azelaic acid is a relatively common constituent in both urban and marine regions.[31,155] Because diacids with odd number of carbon atoms are highly soluble in water, they are considered to be the major contributor to the CCN activity of organic aerosols. Chemical analysis of aerosol collected over the Mediterranean Sea showed that higher ratios of azelaic acid to unsaturated fatty acids were concurrent with higher ozone concentrations, in accord with the proposed reaction mechanism.[156]

3.5.4. Summary for Ozone-Proxies Reactions

Reactions of ozone with unsaturated aerosol-associated compounds result in the formation of both volatile and nonvolatile products. The volatile products are aldehydes of various chain lengths, depending on the position of the double bond in the parent molecule. Laboratory studies demonstrated the formation of aldehydes such as formaldehyde, nonanal, hexanal, and nonenal. These aldehydes can photolyze in the troposphere or react with the OH radical.[157] The products that remain in the aerosol phase are mostly carbonyls, carboxylic acids, and diacids. The surface-bound products modify the surface properties and make the surface more hydrophilic. The remaining surface aldehydes and carbonyls can potentially absorb solar radiation, thereby affecting the optical properties of aerosols and their direct climatic effects. The dicarboxylic acids that remain in the aerosol phase are water-soluble and therefore can affect the ability of processed organic aerosols to act as cloud condensation nuclei, which modifies the aerosol indirect climatic effects. The phase of the aerosol, i.e., solid or liquid, determines the magnitude of the uptake and the yields of the products. Aerosol phase is an important parameter that should be considered when modeling the chemistry and growth of organic aerosols.

3.5.5. Kinetic and Mechanistic Studies of Ozone Uptake Using Aerosol Flow Tubes

In addition to liquids and surfaces, recent aerosol flowtube experiments were also carried out for study-

ing the chemistry of organic aerosols. These experiments commonly employ techniques that probe the changes in the chemical composition of the aerosol, rather than monitoring the gas-phase reactant.

Pöschl et al.[76] investigated the interaction of ozone and water vapor with soot particles coated with benzo[*a*]pyrene (BaP), a five-ring polycyclic aromatic hydrocarbon. The study was carried out in an aerosol flowtube experiment at ambient temperature and pressure.[76] The BaP surface coverage was kept at ~0.2 monolayer. The ozone volume mixing ratio varied between 0 and 1 ppm and the RH between 0 and 25%. The pseudo-first-order decay rate of BaP in collected particles was determined using HPLC. The observed pseudo-first-order BaP decay rate coefficients exhibited a Langmuir-type dependence on the gas-phase ozone concentration, as shown in Figure 12.

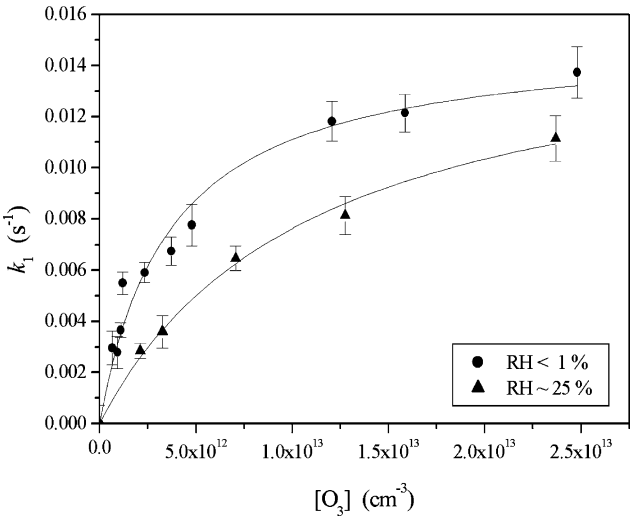

Figure 12. The dependence of the BaP loss rate on ozone concentration. Reprinted with permission from ref 76. Copyright 2001 American Chemical Society.

The loss rates of BaP decreased in the presence of water vapor. This indicates rapid, reversible, and competitive adsorption of O_3 and H_2O on the particles followed by a slower surface reaction between adsorbed O_3 and BaP. The apparent reaction probabilities of BaP due to reaction with ozone have been calculated on the basis of the BaP loss:

$$\gamma_{\mathrm{BaP}} = \frac{4}{\sigma_{\mathrm{BaP}}\omega_{O_3}}\frac{k_s^{1}}{[O_3]} \qquad (8)$$

where σ_{BaP} is the cross section of the BaP molecule, ω is the mean thermal velocity of ozone, k_s^1 is the pseudo first-order loss rate of BaP, and [O_3] is the ozone gas-phase concentration. A plot of γ_{BaP} versus ozone concentration shows a decrease of γ as a function of gas-phase ozone concentration (see Figure 13) and further a decrease due to competitive adsorption of water. This behavior is explained by the Langmuir−Hinshelwood reaction mechanism (see section 4).

On the basis of measurements of ozone and BaP losses, it was possible to derive the basic physicochemical parameters that govern the multiphase loss

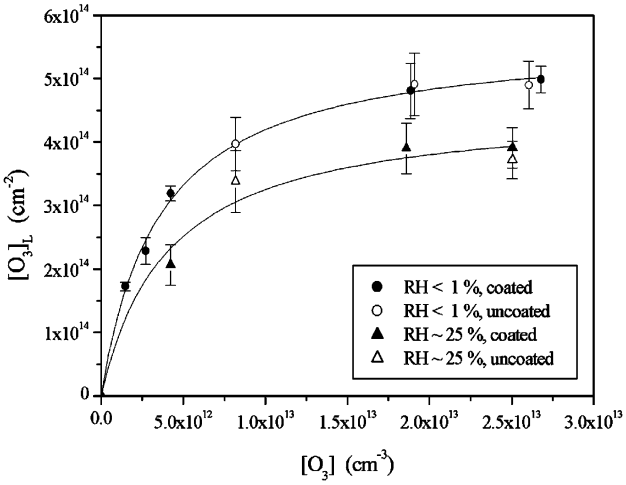

Figure 13. The decrease in the reactive uptake coefficient due to increase in the ozone mixing ratio. Reprinted with permission from ref 76. Copyright 2001 American Chemical Society.

process (see also derivation in section 4): O_3 and H_2O Langmuir adsorption equilibrium constants $K_{O3} = (2.8 \pm 0.2) \times 10^{-13}$ cm^3 and $K_{H2O} = (2.1 \pm 0.4) \times 10^{-17}$ cm^3, maximum pseudo-first-order BaP decay rate coefficient $k_s^1 = (0.015 \pm 0.001)$ s^{-1}, and adsorption site surface concentration $[SS]_S = (5.7 \pm 1.7) \times 10^{14}$ cm^{-2}. On the basis of these values, a second-order BaP−O_3 surface reaction rate coefficient $k_s = (2.6 \pm 0.8) \times 10^{-17}$ cm^2 s^{-1} was calculated. Estimates for the mean surface residence times and adsorption enthalpies of O_3 and H_2O have been derived: $\tau_{O3} = 5-18$ s; $\tau_{water} \approx 3$ ms, $\Delta H_{ads,O3} = -(80-90)$ kJ mol^{-1}, $\Delta H_{ads,H2O} \approx -50$ kJ mol^{-1}.[76]

The half-life of surface BaP molecules is about 5 min at 30 ppb O_3 under dry conditions. This is shorter than previous estimates for the BaP atmospheric lifetime. At higher RH and with multilayer BaP surface coverage, however, the BaP half-life was substantially longer. The longer lifetime is attributed to competitive H_2O adsorption and to shielding caused by accumulation of products on the surface. For example, at 30 ppb O_3 and 25% RH, the lifetime increased to 18 min and to 44 min at 75% RH.

Extrapolation of the parameters derived in this work to the atmosphere should be done with care. On the one hand, BaP molecules in the bulk of the particles may not be similarly exposed to ozone as the surface BaP molecules. On the other hand, reactions with other oxidants, such as OH and NO_2, as well as photolysis by solar radiation may shorten the lifetime in the atmosphere. The short lifetimes derived suggest that reactive species such as BaP would not be transported for long distances. This calls for a thorough identification of the reaction products of reactive aerosol organics and their environmental impacts.

New particle mass spectrometers are capable of measuring aerosols' size distribution simultaneously with the determination of their chemical composition.[66,70,71] These instruments open possibilities to study aerosol chemical kinetics in flowtubes with online chemical and size analysis. Morris et al.[101] studied the reaction kinetics of submicron oleic acid

aerosols with ozone using an aerosol flowtube coupled to an aerosol mass spectrometer (AMS). A flow of size-selected aerosols was introduced into a flow reactor where the particles were exposed to a known concentration of ozone for a controlled period of time. The aerosol flow was then directed into an aerosol mass spectrometer for particle size and composition analyses. The reaction kinetics was followed by monitoring the disappearance of oleic acid from the aerosols due to its reaction with ozone. In addition, it was possible to obtain quantitative information about the formation of aerosol-phase products. The aerosol-phase reaction products observed were in agreement with the mechanism suggested by Moise and Rudich.[90] No attempt to detect gas-phase products was made. It was found that at least on the time scale of the experiment (seconds) the fractional loss of oleic acid from particles with smaller diameters was larger than that of larger diameter particles. In addition it was observed that the reacted particles had slightly increased in size following reactions. Careful accounting of the total mass, derived from the particles' mass spectra, and the ozone loss, was used to confirm that each oleic acid molecule reacted with only one ozone molecule.

The results were interpreted in terms of a chemical kinetics model for aerosol reactive transformations.[158] Assuming a fast reaction scheme in which the reaction occurs in a thin shell close to the aerosol surface (diffuso-reactive length) the change in oleic acid concentration in the reacted particles could be fit to an equation

$$\sqrt{\frac{[\text{oleic}]_{(t)}}{[\text{oleic}]_0}} = 1 - \frac{3RTn_{\text{ozone}}H\sqrt{D_{\text{ozne}}k_2}}{2a\sqrt{[\text{oleic}]_0}}t \qquad (9)$$

where n_{ozone} is the ozone concentration, H is the solubility constant of ozone in the aerosol, k_2 is the second-order rate coefficient for the ozone-oleic acid reaction, D_{ozone} is the diffusion coefficient of ozone in the aerosol, and a is the aerosol diameter. With this equation it was possible to fit the observed loss of the oleic acid in the different particle sizes using the same set of H, D, and k_2 parameters, even though the loss rates of oleic acid were higher for the smaller particles (Figure 14). Using the derived parameters,

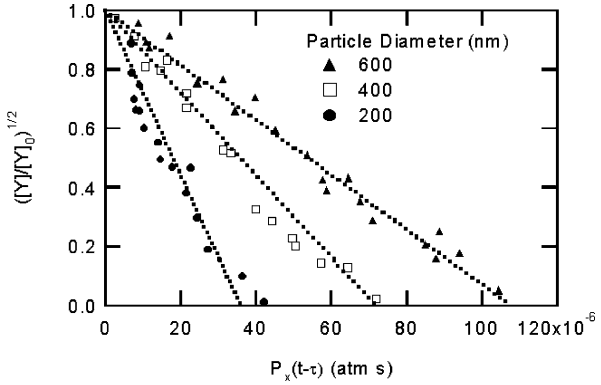

Figure 14. The depletion of oleic acid as a function of time in 200, 400, and 600 nm particles. Reprinted with permission from ref 101. Copyright 2002 American Geophysical Union.

the reactive uptake coefficient for ozone uptake by oleic acid aerosols independent of particle size was obtained, $\gamma = (1.6 \pm 0.2) \times 10^{-3}$.[101] This γ value is about a factor of 2 higher than the value derived by the flowtube experiments.[90,103] A diffuso-reactive length of 10 nm was calculated from this analysis, in agreement with previous estimates.[90]

Smith et al.[102] used a different type of single-particle mass spectrometer coupled to a flowtube to measure the reactive uptake coefficient of ozone by oleic acid aerosol particles. The reaction was again followed by monitoring the decrease of oleic acid in size-selected particles as a function of O_3 exposure. The reactive uptake coefficient was found to depend on the size of the particles, with γ_{meas} ranging from $\gamma = (0.99 \pm 0.09) \times 10^{-3}$ to $\gamma = (7.3 \pm 1.5) \times 10^{-3}$ for particles ranging in diameter from 1.3 to 4.9 μm (see Figure 15). The observed linear relationship between

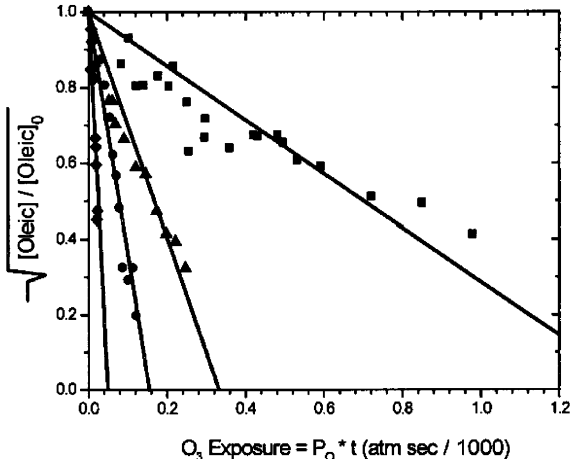

Figure 15. Oleic acid decay profiles as measured with the single-particle mass spectrometer for four particle sizes: ◆ 680, ● 1.38, ▲ 1.86, and ■ 2.45 μm. Though linear fits can be made to each decay independently, no single set of parameters (H, D, and k_2) can fit all of the data simulations. Reprinted with permission from ref 102. Copyright 2002 American Chemical Society.

γ and particle size cannot be easily explained. Specifically, γ cannot decrease below 0 for particles >5 μm and certainly will not increase indefinitely for the small particles.

In addition to the uptake experiments, the appearance of products was monitored at several masses, but only 9-oxononanoic acid and nonanal were identified with confidence. Other products (at m/e = 141, 155, and 171) were not assigned (see Figure 16). A growth in particle aerodynamic size was observed following the reaction. The growth varied linearly with ozone exposure assuming a constant density of the reacted particles.

To explain the observed dependence of the uptake coefficient on the size of the particle, a model for the reactive uptake was constructed. On the basis of this model, it was suggested that the decrease in γ_{meas} with increasing particle size results from the reaction being limited by the diffusion of oleic acid within the particle. On the basis of the measurements and model, a value of $\gamma = (5.8-9.8) \times 10^{-3}$ was estimated for particles that are not limited by oleic acid diffusion. The derived value is higher than other mea-

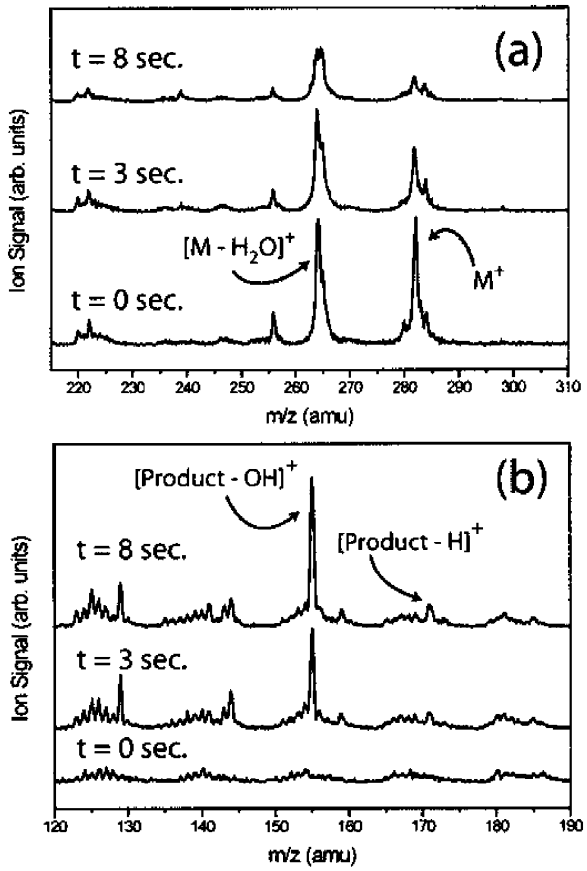

Figure 16. Appearance of products from ozone + oleic acid aerosols, as probed by a single aerosol mass spectrometer. Reprinted with permission from ref 102. Copyright 2002 American Chemical Society.

surements using oleic acid liquids[79,103] or aerosols.[101] The model includes simultaneous diffusion and reaction of both O_3 and oleic acid in the aerosol phase. However, no single set of H and D could be used to fit the behavior of all particle sizes (see Figure 15). The model indicates that oleic acid must diffuse within the particle more slowly than is predicted by the measured oleic acid self-diffusion constant. Therefore, it was proposed that as a result of the reaction, nonreactive ozonolysis reaction products accumulate at the surface and lead to a slower ozone-oleic acid reaction.[102]

The results of Morris et al.[101] and Smith et al.[102] demonstrate the advantages of new aerosol mass spectrometers in studying the chemical reactions of aerosols. Size-selected particles can react, and changes in the aerodynamic size as well as the dependence of the rate of reaction on the size of the particles can be probed simultaneously. Detecting the appearance of products is also feasible with these techniques.

It is not clear why the results of Morris et al.[101] and Smith et al.[102] differ. While Morris et al.[101] fit all the size-dependent data by a single set of constants, this was not possible in the Smith et al.[102] study, and diffusion through a nonreactive layer had to be invoked. It is possible that the reason for the discrepancy lies in the substantially larger particles used in the Smith et al. experiments, which led to the formation of a thicker nonreactive layer.

Oleic acid was measured in urban aerosol and biomass burning particles,[31] and was basically considered an inert tracer. On the basis of the measured uptake coefficients, however, it should be rapidly consumed under atmospheric conditions. The reason for this discrepancy between the laboratory-derived parameters and the field observations is not clear. It is conceivable that the nature of mixed organic and inorganic atmospheric aerosols slows the fast diffusion of ozone (which is lipophilic) into the particles and therefore slows the reaction with oleic acid. It is also possible that competitive adsorption of water slows the reaction, similar to the reaction of ozone with BaP coated soot particles.[76]

Both aerosol flowtube experiments[101,102] measured reactive uptake coefficients which are higher than those measured by the liquid low-pressure experiments.[90,103] The reason for the different values is not completely clear. It may result from the aerosol production process which involves atomizing oleic acid with a solvent such as methanol or propanol. If the solvent does not completely evaporate (0.2 mol fraction in the Morris et al. experiment[101]), the diffusion of ozone in the liquid may be faster than the diffusion of ozone in pure oleic acid, resulting in faster uptake. To resolve this issue, different, solvent-free, techniques for making particles could be used.

A growth in the reacted particles' aerodynamic diameter was observed in both experiments that employed aerosol mass spectrometers. Since the experiments were performed under dry conditions, water uptake can be excluded. This observation contrasts with the observed release of nonanal to the gas phase in the liquid and film experiments,[85,90,103] which suggests that the particles should decrease in size. It is not clear why the two experimental approaches show different behavior. Two possible explanations are that (a) the density of the reacted particles is different leading to changes in the aerosols' time-of-flight, and therefore their derived aerodynamic diameter, or (b) the release of the volatile products occurs on a longer time scale in the liquid and film experiments than in the AMS experiments.

3.5.6. Uptake of OH by Organic Surfaces

Bertram et al.[84] studied the heterogeneous loss of OH ([OH] $\approx 1 \times 10^8$ cm^{-3}) on halocarbon wax, organized organic monolayers (SAM), and several solid organic surfaces (paraffin wax, a mixture of stearic and palmitic acids, pyrene, and soot). These studies used a low-pressure flowtube reactor coupled to a chemical ionization mass spectrometer. A reaction probability of $\gamma > 0.1$ for all the organic surfaces investigated was determined. For halocarbon wax, $\gamma < 1 \times 10^{-3}$. Measurements of the contact angle of water with surfaces exposed for longer times showed a dramatic decrease from 100° to 10°, indicating that the surfaces became very hydrophilic. Since the OH reaction is not selective, even less reactive alkane surfaces showed this behavior. This is in contrast to ozone reactions which are limited to reactions at specific sites, i.e. double bonds, and therefore reacted alkenes surfaces showed only modest decreases in contact angle.[84]

Bertram et al.[84] proposed that the extent of oxidation of the organic aerosol surface can be estimated, assuming that the OH reaction is the rate-limiting step, to be

$$\text{Fraction of surface oxidized} = \exp\left(-\frac{\gamma Z t}{N_{\text{total}}}\right) \quad (10)$$

where γ is the reaction probability, Z is the collision frequency with the surface, t represents the time, and N_{total} is the total number of reaction sites. Using this equation it is calculated that for $5 \times 10^5 < [\text{OH}] < 5 \times 10^6$ cm^{-3}, OH reacts with 90% of the sites in less than 7 days, which is comparable with the residence time of tropospheric aerosols. The time could be shorter due to surface reactions of other oxidants.[84]

Although OH reacts very efficiently on organic surfaces, this is only of minor importance as a sink of OH in the troposphere since it does not compete with fast gas-phase loss processes of OH. This study, however, demonstrates that, similar to other oxidative reactions on surfaces,[69,79,83,85,90,103] the OH-organic heterogeneous reactions will significantly modify the surface properties of organic aerosols and their ability to act as CCN in the troposphere.

Low-vapor-pressure organic compounds will partition mostly on the surface of aerosols.[52,159−161] Because of their negligible gas-phase concentration, reactions with atmospheric oxidants will occur mostly on the surface of particles, and these processes will determine their atmospheric fate. Pesticides and high molecular weight PAH released to the atmosphere are among the species that will have their atmospheric lifetimes and transport determined by reactions on the surface of aerosols.

Zetzsch and co-workers[48,77,107] studied reactions of pesticides adsorbed on SiO_2 inert aerosols with gas-phase oxidants. The experiments were performed in a large smog chamber where both gas-phase and aerosol-phase reactions of these compounds were studied. These experiments demonstrated that the loss of surface-adsorbed pesticides is dominated by reactions with the OH radical. Reactions with other oxidants such as ozone or hydrogen peroxide were found to be orders of magnitude slower, and therefore are not expected to contribute to the atmospheric degradation of aerosol-bound pesticides. On the basis of these studies, the atmospheric half-life of pesticides such as pyrifenox is expected to be less than a day.

The reaction mechanism of the OH degradation of the pesticides was studied by identifying some of the compounds formed by the reaction. It was found that the reaction proceeds through hydrogen abstraction at the methylene group. In the reaction of tertbutylazine (TBA) with OH, it was shown[77] that following the hydrogen atom abstraction, oxygen adds to the resulting alkyl radical. Following reaction of NO with the peroxy radical, a ketone is formed. In addition to these gas-phase-like reactions, it is possible that electron-transfer reactions also play a role in the degradation of some pesticides.

3.5.7. Uptake of NO_2 and $ClONO_2$ by Organic Liquids and Surfaces

The uptake of NO_2 by a solid film of anthrarobin (1,2,10-trihydroxy-anthracene) was studied by Ammann and co workers[75] in a flowtube under atmospheric pressure, 20−80% RH and NO_2 concentrations in the ppb range. Anthrarobin was chosen as a representative of oxy-PAH that originate from biomass burning and fossil fuel combustion. About 2×10^3 monolayers of the PAH were deposited on the surface of a flowtube. A series of traps were installed following the reactor to capture and analyze volatile products released by the reaction. These experiments used ^{13}N labeled NO_2. Due to the high detection sensitivity of ^{13}N, experiments were performed at atmospherically relevant conditions that allow detection of low-yield reaction products.[75,141]

An upper limit of $\gamma \leq 1 \times 10^{-7}$ was found for reactive uptake of NO_2 by the anthrarobin surface. HONO was the only observed product.[75] The HONO yield increased linearly with the NO_2 exposure. The uptake of NO_2 decreased with exposure time, indicating the consumption of reactive sites on the anthrarobin surface. With increasing NO_2 concentration γ decreased, suggesting that the NO_2 uptake on the anthrarobin surface is limited by a fast Langmuir adsorption−desorption equilibrium followed by a slow surface reaction, i.e., reaction following the Langmuir−Hinshelwood mechanism (see Figure 17, section 4). Using a Langmuir−Hinshelwood analysis, physicochemical parameters for the process could be derived. Specifically, a value of $k_s \approx 1 \times 10^{-20}$ cm^2 s^{-1} was found for the surface rate coefficient, $K = 5 \times 10^{-3}$ ppb^{-1} for the Langmuir equilibrium constant, and $N_s = 10^{15}$ cm^{-2} was found for the surface concentration of reactive sites (OH groups). For an explanation of the Langmuir−Hinshelwood mechanism and its applications to surface processes on atmospheric aerosols, see section 4.

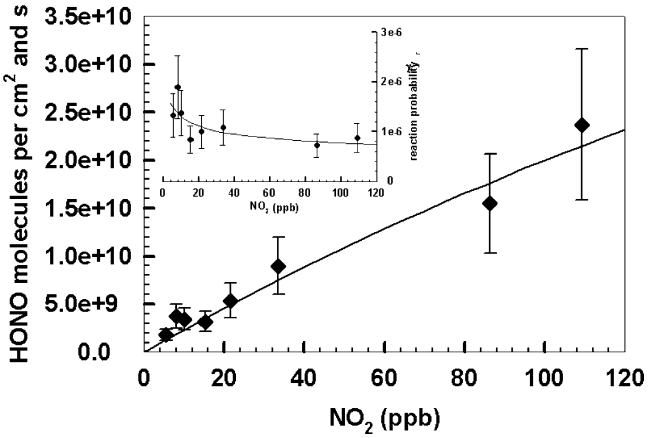

Figure 17. Initial HONO formation rates on anthrarobin coatings (averages of the first 30 min of reaction) as a function of the NO_2 mixing ratio at 26 °C and at 42% relative humidity. The insert shows the corresponding reaction probability γ_r. Reprinted with permission from ref 75. Copyright 2002 Royal Society of Chemistry.

The uptake of NO_2 and the HONO formation rate increased as a function of relative humidity, scaling with a BET adsorption isotherm for water. This behavior indicates that water is an essential partner in the reaction. In addition, an activation energy of 38 kJ mol^{-1} was derived for the overall process.[75]

An overall picture of the NO_2 reaction with anthrarobin is drawn from these experiments: The

reaction between gas-phase NO_2 and solid anthrarobin surfaces leads to release of gas-phase HONO as the main reaction product. Nitration of anthrarobin is not a major reaction channel. The lack of HNO_3 as a reaction product indicates that the disproportionation reaction between NO_2 and water, which forms equal amounts of HONO and HNO_3, is also negligible. The heterogeneous chemical reduction of NO_2 to HONO on anthrarobin surfaces is an activated process that requires energy. The initial reaction rate dependence of NO_2 scales with a Langmuir isotherm for NO_2 and is consistent with a first-order loss of adsorbed NO_2. However, the time-dependent decrease of the HONO formation rate cannot be represented by an approach in which a single reactant is consumed (i.e. by a single-exponential function). Even less clear is the involvement of water in the kinetics; water seems to be necessary for the reaction on the bulk surface as well as for the reaction with submonolayer coverings of anthrarobin deposited on glass.

The suggested reaction mechanism includes an acid−base equilibrium followed by electron transfer

$$ArOH + H_2O \leftrightarrow ArO^- + H_3O^+ \qquad (R2)$$

$$ArO^- + NO_2 \rightarrow ArO^\bullet + NO_2^- \qquad (R3)$$

$$NO_2^- + H_3O^+ \leftrightarrow HONO + H_2O \qquad (R4)$$

It is questionable, however, whether a surface aqueous film can support a mechanism that involves two acid−base equilibria. On the basis of the similarity of the reaction kinetics with the reactive uptake of NO_2 on soot,[141] this work suggests that the reactivity of anthrarobin, which is representative of a category of organics present on soot (i.e. aromatic compounds containing OH-functional groups), may be used as a model for understanding the chemical properties and reactions occurring on soot.

The reactive uptake of $ClONO_2$ by ethylene glycol, cyclohexanone, decanol, and tridecane was studied by Hanson[88] in a low-pressure flowtube coupled to a chemical ionization mass spectrometer. It was found that the $ClONO_2$ loss was limited by diffusion in the gas-phase. Therefore, only a lower limit of $\gamma > 0.06$ for all liquids was reported.[88] The main observed product was HNO_3, which was released to the gas phase, with a 30% yield for uptake by tridecane. HOCl production was not observed. Since HNO_3 is the major product of the reaction, it is likely that the liquid-phase products are chloroalkanes. Hanson suggested that the likely reaction mechanism of $ClONO_2$ with the organic liquid is

$$Cl{-}ONO_2 + R{-}H \rightarrow HONO_2 + Cl{-}R \qquad (R5)$$

This reaction is probably exothermic by 40−45 kcal mol^{-1}.[88] The suggested reaction mechanism has several important implications: First, $ClONO_2$ can be lost by direct reaction not involving dissociation or ionization. Second, the loss of $ClONO_2$ on organic coated aerosols, especially in dry environments where hydrolysis is low, could be very efficient. Finally, the reaction product HNO_3 is a more stable NO_x reservoir than $ClONO_2$[88] and is expected to remain in the aerosol phase. Therefore, this reaction may be a NO_x removal channel.

3.5.8. Uptake of NO_3 by Organic Liquids and Surfaces

The reactive uptake of the NO_3 radical by liquid and frozen organics was studied by Moise et al.[91] in a rotating wall flow tube coupled to a White cell. NO_3 was detected by a diode laser system at 662 nm. The organic liquids used covered the common functional groups which are found in aerosols: *n*-alkane, *n*-alkenes, carboxylic acids, alcohol, and conjugated alkenes. The reactive uptake coefficients (γ) of NO_3 on n-hexadecane, 1-octadecene, 1-hexadecene, *cis*+*trans*-7-tetradecene, *n*-octanoic acid, 2,2,4,4,6,8,8 heptamethyl nonane, 1-octanol, *cis*,*trans*-9,11- and 10,12-octadecadienoic acid, and *cis*-9,*cis*-12 octadecadienoic acid varied from 1.4×10^{-3} to 1.5×10^{-2}. The uptake coefficients of NO_3 by n-hexadecane and *n*-octanoic acid decreased by a factor of ~5 upon freezing, suggesting that the reaction occurs in the bulk of the organic liquid as well as on the surface. Upon freezing, no diffusion and solvation of the NO_3 into the bulk occurs, and the reaction is limited to the surface layers and therefore γ decreases. For the rest of the compounds studied, no significant change in values of γ was observed upon freezing of the liquids. These conclusions are corroborated by estimation of the diffuso-reactive length and solubility constant of NO_3 in these liquids. The uptake measurements were used to estimate $H\sqrt{(D_l k_l^I)}$ as well as the solubility of NO_3 in the organic liquid, using the relationship

$$\gamma = \frac{4RT}{\omega} H \sqrt{D_l k_l^I} \qquad (11)$$

where D_l ($cm^2\ s^{-1}$) is the diffusion coefficient of NO_3 in the organic liquid and k_l^I (s^{-1}) is the first-order loss rate of NO_3 in the liquid. On the basis of the diffusion coefficients of different inorganic compounds in *n*-hexane and other solvents[162] an average value of $D_l = 2 \times 10^{-5}$ $cm^2\ s^{-1}$ for the diffusion coefficient of NO_3 in organic liquids was chosen. The rate coefficient for NO_3 in liquid was estimated on the basis of its gas-phase rate coefficients to be $k_l = 6 \times 10^4$ $M^{-1}\ s^{-1}$. Using the measured $\gamma = 2 \times 10^{-3}$ for n-hexadecane at 292 K, $H\sqrt{(D_l k_l^I)} = 0.84$ M cm atm^{-1} s^{-1} and $H \approx 0.8$ M atm^{-1} (the activity of a pure organic liquid was taken to be 1). This solubility constant is of the same order of magnitude as the solubility determined for NO_3 in water (0.6 ± 0.3 M atm^{-1}).[163]

The reactivity in the bulk liquid could be the result of this limited solubility, and thus NO_3 could react to a depth equal to the diffuso-reactive length, *l*, in the liquid. This length is defined as[164]

$$l = \sqrt{\frac{D_l}{k_l^I}} \qquad (12)$$

The diffuso-reactive length is estimated by assuming the same values as for the calculation of the solubility constant. For hexadecane, a derived value of $l \approx 1 \times$

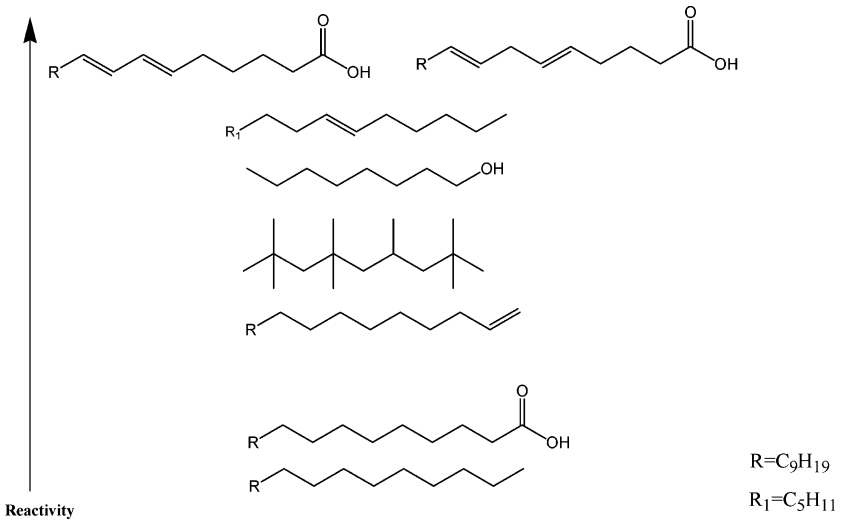

Figure 18. The trend of NO_3 reactivity toward frozen organic liquids. Reprinted with permission from ref 91. Copyright 2002 American Geophysical Union.

10^{-5} cm indicates that the reaction occurs much deeper than the first couple of surface layers. This explains the decrease upon freezing. For alkenes, assuming a gas-phase rate coefficient of $k = 1 \times 10^{-13}$ cm^3 $molecule^{-1}$ s^{-1}, one finds that in the liquid phase, the rate coefficient for reaction of octadecene with NO_3 would be $k_l^I = 6 \times 10^8$ M^{-1} s^{-1}, yielding $l \approx 6 \times 10^{-7}$ cm. The derived length is on the order of a few molecular layers. This is consistent with the reaction occurring very close to the surface of the organic layer, rather than in the bulk.

The observed reactivity of the frozen liquids correlated qualitatively with the known gas phase reactivity for the majority of the compounds studied here, i.e., the uptake by the more reactive compounds occurred mostly on the surface and contribution from solvation and reaction in the bulk was negligible.[91] The reactivity trend of the organics is shown in Figure 18. The least reactive are the *n*-alkane and the octanoic acid. The reactivity increases with the addition of more reactive functional groups, such as a double bond. As the liquid changes from 1-alkene to an alkene with two double bonds, the reactivity further increases. Within the uncertainty associated with high γ, the uptake coefficient of a molecule with two conjugated double bonds is similar to that of a molecule with two nonconjugated double bonds. It is also seen that the branched alkane (heptamethyl nonane) is more reactive than the *n*-alkane, and the substituted alkene (7-tetradecene) is more reactive than the terminal alkenes. This trend is consistent with the known gas-phase reactivity of NO_3 (alkane < branched alkane, alkane < alkene, terminal alkene < substituted alkene, alkene < diene).

3.5.9. Uptake of Cl and Br by Organic Surfaces

High concentrations of Cl and Br, $\sim 10^5$ [165] and $\sim 10^6$ atoms cm^3, respectively, are estimated for marine environments where high organic aerosol concentrations are also expected.[35,166,167] The reactive uptake of Cl and Br atoms by closely packed organic thin films was studied in a low-pressure flow reactor by Moise and Rudich.[83]

The uptake coefficients due to reactive uptake by SAM of alkene were measured at room temperature and in the presence of oxygen and are shown in Table 3. For Br, $\gamma = (3 \pm 1) \times 10^{-2}$ for an alkane surface

Table 3. Reactive Uptake Coefficients of Various Radicals and Oxidants on a Surface of Alkanes and Alkenes[79,83]

oxidant	γ alkane monolayer	γ alkene monolayer
O_3	$<10^{-6}$	1.0×10^{-4}
Cl ($+O_2$)	>0.1	>0.1
Br ($+O_2$)	3×10^{-2}	5×10^{-2}
O (^3P)	1.0×10^{-2}	20.0×10^{-2}

and $\gamma = (5 \pm 2) \times 10^{-2}$ for alkene surfaces.[83] Cl was more reactive with $\gamma \geq 0.1$. The processing of the surface was monitored using FTIR, XPS, and contact angle measurements. Surface-bound products were determined, and changes in the surface hydrophobicity were measured. The contact angles of water decreased by more than 50° following the reaction, indicating a substantial change in surface order, morphology and hydrophobicity. The IR vibrational lines of C═C, CH_3, and CH_2 which were observed clearly by direct IR absorption prior to exposure nearly completely disappeared.

Surface analysis with XPS following exposure did not show the presence of the halogens on the surface, suggesting that halogenated reaction products are released to the gas phase. This agrees with the observed ~20% reduction in film thickness. 50−60% of the remaining carbon on the surface is assigned to methylene chains. The remaining carbon became progressively more oxidized as was evident from the shift of the C (1 s) line from its characteristic energy at 285 eV. Similar shifts were observed for both the Cl and Br reactions.[83] Analysis of the chemical species depth distribution was conducted by varying the angle between the source X-ray beam and the sample. Using this technique, it was inferred that the oxidized carbon sites are located mostly at the upper layer of the remaining organic surface. The shift of 4.5 eV observed in the XPS spectrum is associated

with the formation of a carboxyl group, specifically carboxylic acid.[168] It was calculated that the number of oxygen atoms bound to a terminal carbon is, on average, greater than 1 per carbon atom, also consistent with acid formation.

The overall emerging picture is that the reaction of the halogen atoms with the organic layers proceeds by hydrogen abstraction and that there is a substantial release of products to the gas-phase. Gas-phase products were not probed by Moise and Rudich.[83] Because the reactive sites are not specific and any C−H bond is in principle a reactive site, the reaction does not show saturation on the time scale of the experiments, similar to OH reactions,[84] and in contrast with reactions of ozone which are limited by the concentration of double bonds[79] or NO_2 reactions with anthrarobin which are limited by the number of available OH groups.[75] This reaction scheme explains the decrease in surface thickness upon reaction and the presence of oxidized products on the upper layers of the reacted surface. This "violent" reaction results in a corrugated and substantially oxidized surface, as reflected by the significant reduction of the contact angle of water. Surfaces that reacted with halogen atoms become much more hydrophilic compared with the ozone reaction with surfaces of terminal alkenes

4. A Langmuir–Hinshelwood Model for Aerosol Surface Reactions

On the basis of many experimental studies, it can be concluded that reactions on the surface of aerosols in general,[169−174] and on organic surfaces in particluar,[75,76,99,141] proceed via a reversible absorption/Langmuir−Hinshelwood mechanism. Steady-state reactive uptake processes driven by reactions in liquid particles have been described using a "resistor" model in which mass accommodation (α) and reaction in the bulk (Γ_b) are added up as separate resistances.[68,175] In this "resistor model" framework, the reactive uptake coefficient of a species X, γ, is formulated in terms of physicochemical parameters such as the solubility (H, M atm^{-1}), the liquid-phase diffusion coefficient (D_l, cm^2 s^{-1}), and the first-order loss rate coefficient of species X in the liquid

$$\frac{1}{\gamma} = \frac{1}{\alpha} + \frac{1}{\Gamma_b} = \frac{1}{\alpha} + \frac{\omega}{4RTH\sqrt{D_l k^I}\left[\coth\left(\frac{r}{l}\right) - \frac{l}{r}\right]} \quad (13)$$

where R is the gas constant and T is the temperature. In the case of a second-order reaction with an aerosol-phase reactant Y, the first-order loss rate coefficient is expressed as $k^I = k^{II}[Y]$ (s^{-1}), where k^{II} is the bulk phase second-order reaction rate coefficient (M^{-1} s^{-1}). The particle radius is r, and l is the diffuso-reactive length (eq 12), which is the depth of the layer in which reaction takes place. l is determined by competition between diffusion and reactive loss. ω is the average thermal speed of the gas-phase reactant.

While reactions in the bulk are well characterized in terms of solubility, concentrations and rate coefficients, the kinetics of surface reactions are generally different from those within a bulk liquid, and their description is much less developed. This led to development of an expression for the reactive uptake coefficient, γ, for the loss of a gas-phase species due to a surface reaction. The model was developed assuming a model which includes reversible adsorption and reaction on the surface followed by a slower surface reaction.[137−139] This expression is based on an application of the Langmuir−Hinshelwood reaction mechanism between one gas-phase and one surface-bound species to atmospheric multiphase processes. The expression for the uptake coefficient, γ, which is defined as the probability that a collision of X with a particle that has a surface concentration of $[Y]_s$ leads to its net uptake into the condensed phase, is shown to be[137]

$$\frac{1}{\gamma} = \frac{1}{S_0} + \frac{1}{\Gamma_s} \quad (14)$$

$$\frac{1}{\Gamma_s} = \frac{1}{k_s^1}\left[\frac{k_d}{S_0} + \frac{\sigma[X]\omega}{4}\right] = \frac{\omega\sigma(1 + K[X])}{4k_s[Y]_s K} \quad (15)$$

In cases where $S_0 \gg \Gamma_S$

$$\gamma = \frac{4k_s[Y]_s K}{\omega\sigma(1 + K[X])} \quad (16)$$

The physicochemical parameters driving the uptake process are as follows: S_0, the surface accommodation coefficient, which is the probability that X adsorbs to the surface, i.e. neither immediately bounces off nor reacts upon collision with the surface; k_d, the desorption rate constant, i.e. the inverse of the surface residence time in the absence of reaction; σ, the area that one adsorbed molecule of X covers; k_s^1, the first-order loss rate in the aerosol phase; k_s, the rate constant of the bimolecular surface reaction. The second expression of eq 15 uses the Langmuir constant, K, defined as the ratio of adsorption and desorption rates coefficients, $K = k_a/k_d$. The expression for Γ_s, the reactive loss on the surface, is similar to previously derived expressions,[138,139] and it can be directly incorporated into the resistor model for surface specific reactions.[176] Figures 19 and 20 show

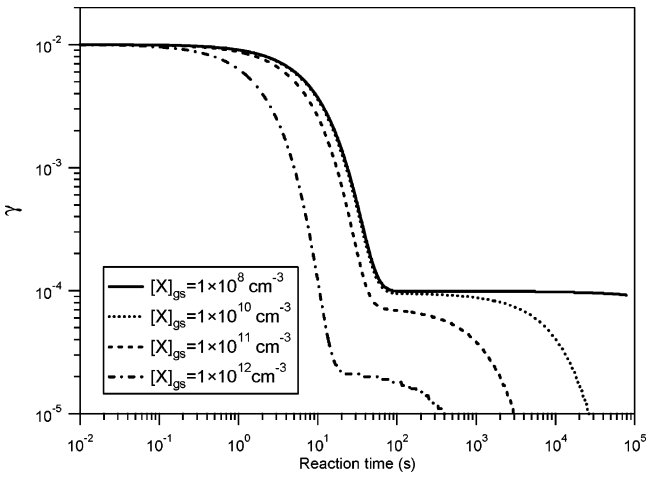

Figure 19. γ_x as a function of time for different gas-phase concentrations according to eq 13. The curves are obtained by numerical integration of the system with the initial concentration of Y set to 1×10^{14} cm^{-2}, $k_s = 1 \times 10^{-17}$ cm^2 s^{-1}, $S = 0.01$, $\tau = 10$ s, $\sigma = 4 \times 10^{-15}$ cm^2.

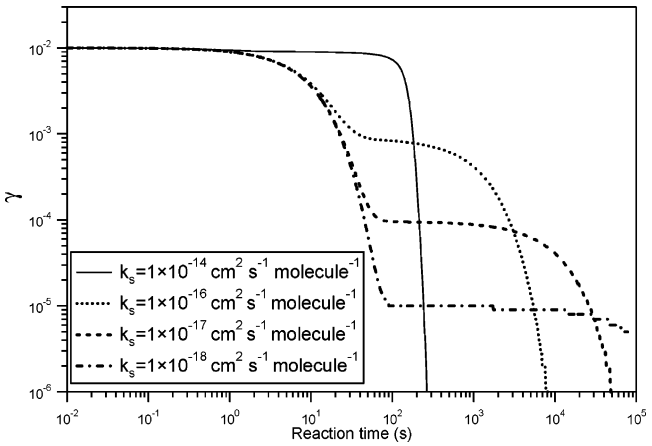

Figure 20. γ_x as a function of time for different values of surface reaction rate coefficient, k_s. The curves are obtained by numerical integration of the system with the initial concentration of Y set to 1×10^{14} cm^{-2}, $[X]_g = 1 \times 10^{10}$ cm^{-3}, $S = 0.01$, $\tau = 10$ s, $\sigma = 4 \times 10^{-15}$ cm^2.

numerical integrations for a range of parameter values to demonstrate that γ varies strongly with time and with the gas-phase concentration of X under conditions typical of atmospheric or laboratory systems.

Several implications of eq 16 are significant in the context of organic aerosol chemistry:

(1) In cases of diffuso-reactive uptake by liquid aerosols, the loss rate is proportional to the square root of the concentration in the bulk phase, $[Y]^{1/2}$.[68,175,177] In surface reactions, under the conditions of the model, eq 16 demonstrates that the loss is directly proportional to the surface concentration of the reactant, $[Y]_s$. The bimolecular rate law has been demonstrated to apply to ozone loss on Benzo-[*a*]pyrene[76] and to the reaction of NO_2 with solid anthrarobin (1,2,10-trihydroxy-anthracene).[75] Typical values of k_s obtained from fits as shown in Figure 13, or from the observed loss rate derived from ozone uptake on organic surfaces, range between 10^{-15} and 10^{-20} cm^2 s^{-1}.[75,76,79]

(2) When replacement of the surface-bound species, Y, from the gas or the aerosol phase is slower than its loss rate due to reaction, $[Y]_s$ is limited. In most laboratory or real systems, the number of surface molecules is much lower than the number of potential reactants in the bulk of particles. Therefore, the depletion of Y in such a surface-limited system occurs more rapidly than in the bulk reaction. As a result, γ decreases with time on relatively short time scales and eventually approaches zero (as demonstrated in the simulation shown in Figure 19). An example is the loss of ozone on a surface containing terminal alkenes.[79] Equation 16 is not applicable to cases where there is significant replenishment of Y from the bulk or from the gas phase, which may be important for surface reactions where the surface reactant is also a bulk species that diffuses rapidly to the surface.[101] Fast replenishment is not likely for reactions of species adsorbed from the atmosphere on short time scales. In these systems, the time dependence for the depletion of Y due to reaction provides a convenient way to calculate the atmospheric lifetime of adsorbed species such as PAHs and pesticides and the processing time of solid particles.

(3) Equation 16 also implies that γ depends on the gas-phase concentration of the reactant $[X]_g$. The relative magnitudes of the adsorption, desorption, and surface rate coefficients will determine at what concentration this effect is significant. Once $K[X]_g \gg 1$, γ will depend inversely on $[X]_g$. This phenomenon directly results from the finite number of surface adsorption sites of X ($\approx 1/\sigma$), which determine the Langmuir equilibrium constant, K. The study of ozone uptake by PAH-coated soot particles[76] shown in Figure 13 or the study of NO_2 uptake by soot and functionalized PAH surfaces[75,141] demonstrate the dependence of γ on the gas-phase concentration at atmospherically relevant conditions. Laboratory experiments performed at even higher gas-phase concentrations are thus likely to be influenced by saturation effects, and care should be taken when using the laboratory-derived parameters to model these processes in the atmosphere. However, if the basic physical parameters are known, γ can be calculated in those models.

(4) Due to the reaction and depletion of the surface molecules, the organic surface becomes more corrugated and oxidized. This by itself could modify the Langmuir equilibrium constant K and, as a result, the number of available reaction sites due to enhanced absorption of water and competition on available adsorption sites. This complex dependence of K on the surface properties is somewhat similar to changes in the solubility constant of some atmospheric species due to changes in pH or ionic strength. At the moment, methods to account for changes in K due to surface modification do not exist.

The derived expression shown in eqs 15 and 16 for γ makes it possible to correctly include surface processes in chemical models and to account for reactive transformations of aerosol-adsorbed species.

5. Summary

It is now widely recognized that organic matter in atmospheric aerosols plays crucial roles in the Earth climate system, the environment and in issues related to humans' health. The importance of aerosols has led to a major effort directed toward understanding the chemistry and physics of aerosols in general and of organic aerosols in particular. One of the major difficulties in studying organic aerosols is the large number of different organic species that are found in atmospheric particles. The organic species cover many different chemical classes and hence they exhibit very different behavior and properties. In addition, organic material is found in all particle states, liquid, solid, and on the surface, each with its own thermodynamic and chemical properties. Mixing with inorganic material introduces additional complexity.

Due to the complexity of organic aerosols systems and their heterogeneous nature, it has been, so far, difficult to identify key chemical reactions and processes that are the most important for quantifying the climatic and the environmental impacts of or-

ganic aerosols. As a result, research has been confined to model systems that mimic at least some of the properties of the real environmental matrix and included species that were either detected in aerosols or possess properties similar to those of identified compounds. The literature survey presented in this review opens a window to these model systems and to the major questions that guided these investigations:

(1) Determination of rate coefficients and reaction mechanisms of chemical reactions pertinent to the transformations of organic material in atmospheric aerosols.

(2) Understanding the role of water uptake on the properties of organic aerosols and the role of the organic layers.

(3) The roles and effects of thin organic layers on the properties of aerosols and cloud droplets.

(4) The effects of an organic layer on mass transfer into particles.

Some specific conclusions about the chemistry of organic matter in aerosols can already be drawn from the studies conducted so far with the simplified model systems:

(a) Reactions with atmospheric oxidants and radicals result in more hydrophilic particles.

(b) The oxidation reactions lead to release of volatile products to the gas-phase and produce water-soluble species that remain in the aerosol phase.

(c) Several reaction mechanisms of atmospheric oxidants and organic matter were characterized, and the role of reactions on the surface versus reactions in the bulk of the particles is better understood.

(d) There is a broad characterization of the organic compounds that absorb water and can potentially act as cloud condensation nuclei. It follows that most organic aerosols and especially those that are mixed with even a small fraction of soluble inorganic matter can act as CCN, even though their growth maybe somewhat slowed.

(e) Surface-bound organic compounds affect mass transfer into and out of particles. They also reduce the surface tension of cloud droplets.

(f) Oxidation reactions on surfaces of atmospheric particles can determine the atmospheric lifetime of adsorbed organics and are essential for understanding and characterizing the degradation pathways of pollutants adsorbed on the particles. This is especially true for the oxidation products of the adsorbed organics, which may have more serious environmental effects than the parent compounds.

The preliminary laboratory studies have made it possible to include, to some extent, the effects of organic matter in atmospheric models. It is now clear that detailed measurements of organic aerosols in the atmosphere will help to constrain and quantify the conclusions from the laboratory studies and define the next generation of scientific questions.

6. Suggested Future Research

In view of the new field measurements and laboratory studies it is important to think about further studies that will broaden our understanding of organic aerosols chemistry and physics. Following are speculations about and recommendations for focus points for future research.

(1) Better characterization of prevalent organic compounds and the inorganic aerosol constituents associated with them, as well as the phase of common aerosol types, will enable laboratory experiments to be conducted with more realistic models. These characterizations will direct laboratory experiments to the following relevant questions:

(a) what chemical reactions should be studied to explain the presence of specific compounds in ambient aerosols,

(b) which phases and phase transitions should be studied,

(c) are the aerosols wet or solid,

(d) what are the needed thermodynamic properties.

The works of Fuzzi et al.[80] and Maria et al.[81] are fundamental in their effort to devise a representative organic matrix that models organic water soluble material and the organic component in aerosols. More studies in this direction are needed. The field observations are crucial for constraining and testing the conclusions drawn from the laboratory studies.

(2) Understanding the role of organic layers. Of special interest is the occurrence and chemical properties of organic layers and surfactants, especially for aqueous droplets. Chemical characterization and reactivity of organic layers will direct further research to their effects on surface tension, mass transfer and how chemical reactions modify the layers' properties. The effect of organic layers on aerosol activation is another important topic to explore.

(3) Systematic studies. Because many different organic species are found in aerosols, it is important to conduct systematic studies that relate chemical properties with aerosol properties. For example, experiments on water uptake and aerosol activation as a function of chain length and branching of dicarboxylic acids or as a function of solubility or packing would be very helpful in drawing general conclusions about aerosol chemistry.

(4) Uptake of water and activation of aerosols containing organic matter. This is an important topic directly related to the aerosols' indirect climatic effects. A better characterization of the process and the parameters that control it are required to effectively model cloud droplet growth and size distribution. Specific topics of interest are:

(a) what is the role of the water-soluble and water-insoluble organic matter,

(b) which organic compounds are the most likely to affect water uptake and droplet growth,

(c) how does chemical processing affect particle activation.

(5) Optical properties. The absorption and scattering of radiation determine the aerosols' direct climatic effects. Better characterization of the optical properties and how they depend on the aerosols age and humidity will be essential for better constraining their climatic effects.

(6) Aerosol-phase chemistry plays a role in determining the atmospheric lifetime of low vapor pressure pollutants, the mechanisms leading to pro-

duction of secondary pollutants, and the mechanisms that lead to formation of water-soluble material. Reactions following the initial oxidation steps have not yet been studied in detail. Important questions in this respect are whether processed organic aerosols can sequester NO_x through reactions of NO_x with the surface radicals, what the reaction products are and whether they are optically active or environmentally benign. More studies directed at identifying products of chemical reactions will help to develop appropriate chemical mechanisms and to see where they differ from the gas-phase chemical processes. Field measurements will be essential for identifying these products in ambient particles, since the field data would serve to constrain the laboratory-derived chemical mechanisms.

(7) Studies of multicomponent aerosols. Most studies so far focused on a single component proxy for organic aerosols. Most aerosols, however, are multicomponent, such as mineral dust coated by organics, soot particles coated by organic matter etc. Therefore, studies that involve multicomponent aerosols are needed. Such studies will probe the effect of the core on the type of adsorbed organics, whether the core affects the chemical processes that occur, and whether dissolution of the core due to water adsorption can change the reaction mechanisms and cloud nucleating properties.

(8) Competitive adsorption and multiple reactions are the more likely situation in the real atmosphere. More theoretical and experimental information is needed to understand these processes. This knowledge will enable incorporation of laboratory-derived parameters into meaningful atmospheric calculations.

(9) Surface photochemistry of adsorbed organic organics.

(10) Chemistry and physics of a surface aqueous layer. Experiments have suggested that a thin water layer or microdroplets can form on the surfaces of organic particles. Experiments probing the effect of such thin water-like film, its properties and chemical transformation on the interface would be desirable.

7. Acknowledgment

Paul Davidovits and Greg Frost are greatly appreciated for helpful comments and suggestions.

8. Glossary

Absorption—The process by which molecules are taken up by the bulk of a medium.

Activation—The spontaneous growth of a droplet when the supersaturation is beyond the vapor pressure according to Raoult Law (i.e. depression of vapor pressure due to dissolved substance) that compensates for the vapor pressure enhancement due to the curvature of the surface (i.e. the Kelvin effect which leads to the increase of vapor pressure due to droplet curvature). After this condition is reached, a droplet will grow spontaneously if the ambient supersaturation remains at or above the respective equilibrium value.

Adsorption—The adhesion of molecules to the surfaces of solid bodies or liquids with which they are in contact.

Albedo—The ratio of the outgoing solar radiation reflected by an object (the Earth, clouds) to the incoming solar radiation incident upon it.

Cloud condensation nuclei (CCN)—Aerosols that can activate and grow to fog or cloud droplets in the presence of a supersaturation of water vapor.

Contact angle—The angle formed at a point on the line of contact of three phases, by the tangents to the curves obtained by intersecting a plane perpendicular to the line of contact with each of three phases. One of the phases must be a liquid, another phase may be solid or liquid and the third phase may be gas or liquid. Contact angle measures the wettability of a surface. A surface which is readily wetted by water is called hydrophilic and a surface which is not is called hydrophobic.

Deliquescence—The sudden transition of a solid substance into a solution as a result of absorption of water vapor from the air.

Differential mobility analyzer (DMA)—An instrument built of two charged concentric cylinders with an inlet slit and a sampling slit. The DMA separates particles based on their electrical mobility. Aerosol particles to be sized are inserted into the annular region between the two cylinders at the inlet slit. They are carried by clean air flowing through the annular region. Particles with mobilities in a certain narrow range are sampled at the sampling slit.

Heterogeneous and multiphase chemistry—Atmospheric chemical reactions which occur in the presence of two or more phases, such as gas + liquids or gas + solids. A distinction between reactions on solids (**heterogeneous reactions**) and those occurring in liquid droplets (**multiphase reactions**) is often made.

Inverse micelle—Micelles are colloids of molecules that have spatially distinct polar and nonpolar parts. In aqueous solutions, the molecules arrange in colloids, directing their hydrophobic part inward and exposing their polar part to the polar aqueous medium. The inverted micelle model is a conceptual description suggested for sea salt particles coated by a layer of hydrophobic organic backbone and a polar ionic group (possibly fatty acids). The term "inverted micelle" means that the polar, hydrophilic ends of the long-chain surfactant are inward toward an ionic brine core and the aliphatic, hydrophobic tails are facing outward to the atmosphere.

Köhler theory—A theory that describes the equilibrium vapor-pressure relationship between liquid solution particles and humid air. The theory predicts the critical size at which the Raoult effect, i.e. depression of vapor pressure due to dissolved substance, balances the Kelvin effect (increase of vapor pressure due to droplet curvature). Above this critical size, a droplet will grow spontaneously if the ambient supersaturation remains at or above the respective equilibrium value.

Mass accommodation coefficient—The probability that a gas-phase molecule striking a liquid will

be incorporated into the liquid.

Molecular controlled semiconductor resistor (MOCSER)—The molecular controlled semiconductor resistor (MOCSER) consists of a doped GaAs layer (50 nm thick) on top of a semi-insulating (Al,Ga)As layer. Because of the space charge in the doped GaAs layer, this semiconductor structure leads to a concentration of maximum electron density at a depth of 30−50 nm from the exposed surface. Therefore, small variations in surface charge lead to considerable changes in carrier concentration within the conductive layer.

Quartz crystal microbalance (QCM)—A gold coated quartz crystal that has a resonant frequency when driven by a small electric current. The resonant frequency changes as matter is deposited on the crystal. The frequency change is directly proportional to the mass change.

Reactive uptake coefficient—The probability that a collision of X with the particle's surface leads to its net uptake into the condensed phase due to reaction. Usually designated by the letter γ.

Self-assembled monolayers (SAM)—A method of forming thin, uniform layers of organic compounds is to take advantage of a process called "self-assembly". This occurs primarily in long chain hydrocarbon molecules adsorbed on surfaces. If the molecules have a dipole moment, the adsorption energy compensates for the dipole−dipole repulsion and allows the formation of a parallel oriented molecular film. The molecules associate into well-ordered domains. This association can lead to the formation of well organized, self-assembled monolayers, called SAM, on surfaces.

SEM-EDX—Scanning electron microscopy (SEM) with energy-dispersive X-ray (EDX) analysis system. Scanning electron microscopy (SEM) is the best known and most widely used of the surface analytical techniques. High-resolution images of surface topography, with excellent depth of field are produced using a highly focused, scanning (primary) electron beam. The analysis of X-rays emitted from the sample provides quantitative elemental information, helping to measure morphology and chemical information on surfaces. Often used for morphological and chemical analysis of single particles collected on different sampling substrates.

Solid-phase microextraction (SPME)—This analytical technique uses a small fused silica fiber coated with an appropriate material such as polydimethylsiloxane. The fiber is held in a syringe-like device. Analytes are extracted from liquid or gas by absorption onto the fiber. The analytes are then thermally desorbed for separation and analysis, usually in a gas chromatograph. No solvents are needed in this process, and analyte extraction and preconcentration are combined in one single step.

Sorption—The combined process of adsorption and absorption.

Supersaturation of relative humidity—Relative humidity is defined as the ratio of the partial pressure of water to its vapor pressure at equilibrium at a specific temperature. Supersaturation is a condition when the partial pressure exceeds the equilibrium pressure.

UNIFAC—A group contribution method that combines the solution of functional groups concept and the UNIQUAC (universal quasi-chemical) model which is a model for calculating activity coefficients. The idea of the group contribution method is that a molecule consists of different functional groups and that the thermodynamic properties of a solution can be correlated in terms of these functional groups. The advantage of this method is that a very large number of mixtures can be described by a relatively small number of functional groups.

X-ray photoelectron spectroscopy (XPS)—In the XPS technique, electrons are emitted from chemical species using X-rays. It is highly surface specific due to the short range of the photoelectrons that are excited from the solid. The energy of the photoelectrons leaving the sample are determined yielding a spectrum with a series of photoelectron peaks. The observed peaks reflect the electron binding energies and are characteristic of each element. The shape of each peak and the binding energy can be slightly altered by the chemical state of the emitting atom. Hence XPS can provide chemical bonding information as well. XPS is not sensitive to hydrogen or helium, but can detect all other elements.

9. References

(1) Pockels, H. *Nature* **1891**, *43*, 437.
(2) Rayleigh, L. *Philos. Mag.* **1899**, *48*, 321.
(3) Jacobson, M. C.; Hansson, H. C.; Noone, K. J.; Charlson, R. J. *Rev. Geophys.* **2000**, *38*, 267−294.
(4) Finlayson-Pitts, B. J.; Pitts, J. N. *Science* **1997**, *276*, 1045−1052.
(5) Lelieveld, J.; Crutzen, P. J.; Ramanathan, V.; Andreae, M. O.; Brenninkmeijer, C. A. M.; Campos, T.; Cass, G. R.; Dickerson, R. R.; Fischer, H.; de Gouw, J. A.; Hansel, A.; Jefferson, A.; Kley, D.; de Laat, A. T. J.; Lal, S.; Lawrence, M. G.; Lobert, J. M.; Mayol-Bracero, O. L.; Mitra, A. P.; Novakov, T.; Oltmans, S. J.; Prather, K. A.; Reiner, T.; Rodhe, H.; Scheeren, H. A.; Sikka, D.; Williams, J. *Science* **2001**, *291*, 1031−1036.
(6) Ramanathan, V.; Crutzen, P. J.; Kiehl, J. T.; Rosenfeld, D. *Science* **2001**, *294*, 2119−2124.
(7) Andreae, M. O.; Crutzen, P. J. *Science* **1997**, *276*, 1052−1058.
(8) Kaufman, Y. J.; Tanre, D.; Boucher, O. *Nature* **2002**, *419*, 215−223.
(9) Haywood, J.; Boucher, O. *Rev. Geophys.* **2000**, *38*, 513−543.
(10) Houghton, J. T.; Ding, Y. *Climate Change 2001*: *The Scientific Basis*; Cambridge University Press: Cambridge, UK, 2001.
(11) Ravishankara, A. R. *Science* **1997**, *276*, 1058−1065.
(12) Baker, M. B. *Science* **1997**, *276*, 1072−1078.
(13) Kunzli, N.; Kaiser, R.; Medina, S.; Studnicka, M.; Chanel, O.; Filliger, P.; Herry, M.; Horak, F.; Puybonnieux-Texier, V.; Quenel, P.; Schneider, J.; Seethaler, R.; Vergnaud, J. C.; Sommer, H. *Lancet* **2000**, *356*, 795−801.
(14) Kaiser, J. *Science* **2000**, *289*, 22−23.
(15) Kaiser, J. *Science* **2000**, *289*, 711−712.
(16) Samet, J. M.; Dominici, F.; Curriero, F. C.; Coursac, I.; Zeger, S. L. *N. Engl. J. Med.* **2000**, *343*, 1742−1749.
(17) Middlebrook, A. M.; Murphy, D. M.; Thomson, D. S. *J. Geophys. Res., Atmos.* **1998**, *103*, 16475−16483.
(18) Murphy, D. M.; Thomson, D. S. *J. Geophys. Res., Atmos.* **1997**, *102*, 6353−6368.
(19) Facchini, M. C.; Fuzzi, S.; Zappoli, S.; Andracchio, A.; Gelencser, A.; Kiss, G.; Krivacsy, Z.; Meszaros, E.; Hansson, H. C.; Alsberg, T.; Zebuhr, Y. *J. Geophys. Res., Atmos.* **1999**, *104*, 26821−26832.
(20) Feingold, G.; Chuang, P. Y. *J. Atm. Sci.* **2002**, *59*, 2006−2018.
(21) Gill, P. S.; Graedel, T. E. *Rev. Geophys. Space Phys.* **1983**, *21*, 903−920.
(22) Charlson, R. J.; Seinfeld, J. H.; Nenes, A.; Kulmala, M.; Laaksonen, A.; Facchini, M. C. *Science* **2001**, *292*, 2025−2026.
(23) Facchini, M. C.; Mircea, M.; Fuzzi, S.; Charlson, R. J. *Nature* **1999**, *401*, 257−259.
(24) Prenni, A. J.; DeMott, P. J.; Kreidenweis, S. M.; Sherman, D. E.; Russell, L. M.; Ming, Y. *J. Phys. Chem. A* **2001**, *105*, 11240−11248.
(25) Jacobson, M. Z. *Nature* **2001**, *409*, 695−697.

(26) Menon, S.; Hansen, J.; Nazarenko, L.; Luo, Y. *Science* **2002**, *297*, 2250−2253.
(27) Crutzen, P. J.; Ramanathan, V. *Science* **2000**, *290*, 1098−1098.
(28) Hoffmann, T.; O'Dowd, C. D.; Seinfeld, J. H. *Geophys. Res. Lett.* **2001**, *28*, 1949−1952.
(29) O'Dowd, C. D.; Jimenez, J. L.; Bahreini, R.; Flagan, R. C.; Seinfeld, J. H.; Hameri, K.; Pirjola, L.; Kulmala, M.; Jennings, S. G.; Hoffmann, T. *Nature* **2002**, *417*, 632−636.
(30) O'Dowd, C. D.; Aalto, P.; Hameri, K.; Kulmala, M.; Hoffmann, T. *Nature* **2002**, *416*, 497−498.
(31) Rogge, W. F.; Mazurek, M. A.; Hildemann, L. M.; Cass, G. R.; Simoneit, B. R. T. *Atmos. Environ.* **1993**, *27*, 1309−1330.
(32) Huebert, B. J.; Charlson, R. J. *Tellus Ser. B−Chem. Phys. Meteorol.* **2000**, *52*, 1249−1255.
(33) Jang, M.; Kamens, R. M.; Leach, K. B.; Strommen, M. R. *Environ. Sci. Technol.* **1997**, *31*, 2805−2811.
(34) Seidl, W. *Atmos. Environ.* **2000**, *34*, 4917−4932.
(35) Ellison, G. B.; Tuck, A. F.; Vaida, V. *J. Geophys. Res., Atmos.* **1999**, *104*, 11633−11641.
(36) Law, N. L.; Diamond, M. L. *Chemosphere* **1998**, *36*, 2607−2620.
(37) Russell, L. M.; Maria, S. F.; Myneni, S. C. B. *Geophys. Res. Lett.* **2002**, *29*, 10.1029/2002GL014874.
(38) Tervahattu, H.; Hartonen, K.; Kerminen, V. M.; Kupiainen, K.; Aarnio, P.; Koskentalo, T.; Tuck, A. F.; Vaida, V. *J. Geophys. Res., Atmos.* **2002**, *107*, art. no. 4053.
(39) Tervahattu, H.; Juhanoja, J.; Kupiainen, K. *J. Geophys. Res., Atmos.* **2002**, *107*, art. no. 4319.
(40) Seinfeld, J. H.; Pandis, S. N. *Atmospheric Chemistry & Physics: From Air Pollution to Climate Change*; John Wiley & Sons: New York, 1998.
(41) Krivacsy, Z.; Gelencser, A.; Kiss, G.; Meszaros, E.; Molnar, A.; Hoffer, A.; Meszaros, T.; Sarvari, Z.; Temesi, D.; Varga, B.; Baltensperger, U.; Nyeki, S.; Weingartner, E. *J. Atmos. Chem.* **2001**, *39*, 235−259.
(42) Zappoli, S.; Andracchio, A.; Fuzzi, S.; Facchini, M. C.; Gelencser, A.; Kiss, G.; Krivacsy, Z.; Molnar, A.; Meszaros, E.; Hansson, H. C.; Rosman, K.; Zebuhr, Y. *Atmos. Environ.* **1999**, *33*, 2733−2743.
(43) Gelencser, A.; Hoffer, A.; Krivacsy, Z.; Kiss, G.; Molnar, A.; Meszaros, E. *J. Geophys. Res., Atmos.* **2002**, *107*, art. no. 4137.
(44) Blanchard, D. C. *Science* **1964**, *146*, 396−397.
(45) Donaldson, D. J.; Anderson, D. *J. Phys. Chem. A* **1999**, *103*, 871−876.
(46) Posfai, M.; Xu, H. F.; Anderson, J. R.; Buseck, P. R. *Geophys. Res. Lett.* **1998**, *25*, 1907−1910.
(47) Falkovich, A. H.; Schkolnik, G.; Ganor, E.; Rudich, Y. Manuscript in preparation.
(48) Palm, W. U.; Elend, M.; Kruger, H. U.; Zetzsch, C. *Chemosphere* **1999**, *38*, 1241−1252.
(49) Molina, M. J.; Molina, L. T.; Kolb, C. E. *Annu. Rev. Phys. Chem.* **1996**, *47*, 327−367.
(50) Andreae, M. O. *Nature* **2001**, *409*, 671−672.
(51) Bowman, F. M.; Odum, J. R.; Seinfeld, J. H.; Pandis, S. N. *Atmos. Environ.* **1997**, *31*, 3921−3931.
(52) Liang, C. K.; Pankow, J. F.; Odum, J. R.; Seinfeld, J. H. *Environ. Sci. Technol.* **1997**, *31*, 3086−3092.
(53) Falconer, R. L.; Harner, T. *Atmos. Environ.* **2000**, *34*, 4043−4046.
(54) Harner, T.; Bidleman, T. F. *Environ. Sci. Technol.* **1998**, *32*, 1494−1502.
(55) Pankow, J. F. *Abstr. Pap. Am. Chem. Soc.* **1999**, *217*, U733−U733.
(56) Pankow, J. F. *Atmos. Environ.* **1998**, *32*, 1493−1497.
(57) Tobias, H. J.; Docherty, K. S.; Beving, D. E.; Ziemann, P. J. *Environ. Sci. Technol.* **2000**, *34*, 2116−2125.
(58) Tobias, H. J.; Ziemann, P. J. *Environ. Sci. Technol.* **2000**, *34*, 2105−2115.
(59) Ziemann, P. J.; Tobias, H. J.; Docherty, K. S. *Abstr. Pap. Am. Chem. Soc.* **2001**, *221*, 273-ENVR.
(60) Li, P.; Perreau, K. A.; Covington, E.; Song, C. H.; Carmichael, G. R.; Grassian, V. H. *J. Geophys. Res., Atmos.* **2001**, *106*, 5517−5529.
(61) Grassian, V. H. *Int. Rev. Phys. Chem.* **2001**, *20*, 467−548.
(62) Schaff, J. E.; Roberts, J. T. *Langmuir* **1998**, *14*, 1478−1486.
(63) Duncan, J. L.; Schindler, L. R.; Roberts, J. T. *J. Phys. Chem. B* **1999**, *103*, 7247−7259.
(64) Rogge, W. F.; Hildemann, L. M.; Mazurek, M. A.; Cass, G. R.; Simoneit, B. R. T. *J. Geophys. Res., Atmos.* **1996**, *101*, 19379−19394.
(65) Schauer, J. J.; Rogge, W. F.; Hildemann, L. M.; Mazurek, M. A.; Cass, G. R. *Atmos. Environ.* **1996**, *30*, 3837−3855.
(66) Jayne, J. T.; Leard, D. C.; Zhang, X. F.; Davidovits, P.; Smith, K. A.; Kolb, C. E.; Worsnop, D. R. *Aerosol Sci. Technol.* **2000**, *33*, 49−70.
(67) Mmereki, B. T.; Donaldson, D. J. *Phys. Chem. Chem. Phys.* **2002**, *4*, 4186−4191.
(68) Kolb, C. E.; Worsnop, D. R.; Zahniser, M. S.; Davidovits, P.; Keyser, L. F.; Leu, M. T.; Molina, M. J.; Hanson, D. R.; Ravishankara, A. R. In *Progress and Problems in Atmospheric Chemistry*; Barker, J. R., Ed.; World Sci.: River Edge, NJ, 1995; Vol. 3.
(69) Demou, E.; Virsam, D. J.; Donaldson, D. J.; Maker, P. A. *Atmos. Environ.*, in press.
(70) Sykes, D. C.; Woods, E.; Smith, G. D.; Baer, T.; Miller, R. E. *Anal. Chem.* **2002**, *74*, 2048−2052.
(71) Woods, E.; Smith, G. D.; Miller, R. E.; Baer, T. *Anal. Chem.* **2002**, *74*, 1642−1649.
(72) Thomas, E.; Rudich, Y.; Trakhtenberg, S.; Ussyshkin, R. *J. Geophys. Res., Atmos.* **1999**, *104*, 16053−16059.
(73) Treves, K.; Shragina, L.; Rudich, Y. *Atmos. Environ.* **2001**, *35*, 5843−5854.
(74) Wahner, A.; Mentel, T. F.; Sohn, M.; Stier, J. *J. Geophys. Res., Atmos.* **1998**, *103*, 31103−31112.
(75) Arens, F.; Gutzwiller, L.; Gaggeler, H. W.; Ammann, M. *Phys. Chem. Chem. Phys.* **2002**, *4*, 3684−3690.
(76) Poschl, U.; Letzel, T.; Schauer, C.; Niessner, R. *J. Phys. Chem. A* **2001**, *105*, 4029−4041.
(77) Palm, W. U.; Elend, M.; Krueger, H. U.; Zetzsch, C. *Environ. Sci. Technol.* **1997**, *31*, 3389−3396.
(78) Thomas, E. R.; Frost, G. J.; Rudich, Y. *J. Geophys. Res., Atmos.* **2001**, *106*, 3045−3056.
(79) Moise, T.; Rudich, Y. *J. Geophys. Res., Atmos.* **2000**, *105*, 14667−14676.
(80) Fuzzi, S.; Decesari, S.; Facchini, M. C.; Matta, E.; Mircea, M.; Tagliavini, E. *Geophys. Res. Lett.* **2001**, *28*, 4079−4082.
(81) Maria, S. F.; Russell, L. M.; Turpin, B. J.; Porcja, R. J. *Atmos. Environ.* **2002**, *36*, 5185−5196.
(82) Ulman, A. *An Introduction to Ultrathin Organic Films: From Langmuir-Blodgett to Self-Assembly*; Academic: San Diego, 1991.
(83) Moise, T.; Rudich, Y. *Geophys. Res. Lett.* **2001**, *28*, 4083−4086.
(84) Bertram, A. K.; Ivanov, A. V.; Hunter, M.; Molina, L. T.; Molina, M. J. *J. Phys. Chem. A* **2001**, *105*, 9415−9421.
(85) Wadia, Y.; Tobias, D. J.; Stafford, R.; Finlayson-Pitts, B. J. *Langmuir* **2000**, *16*, 9321−9330.
(86) Daumer, B.; Niessner, R.; Klockow, D. *J. Aerosol Sci.* **1992**, *23*, 315−325.
(87) Rudich, Y.; Benjamin, I.; Naaman, R.; Thomas, E.; Trakhtenberg, S.; Ussyshkin, R. *J. Phys. Chem. A* **2000**, *104*, 5238−5245.
(88) Hanson, D. R. *J. Phys. Chem.* **1995**, *99*, 13059−13061.
(89) de Gouw, J. A.; Lovejoy, E. R. *Geophys. Res. Lett.* **1998**, *25*, 931−934.
(90) Moise, T.; Rudich, Y. *J. Phys. Chem. A* **2002**, *106*, 6469−6476.
(91) Moise, T.; Talukdar, R. K.; Frost, G. J.; Fox, R. W.; Rudich, Y. *J. Geophys. Res.* **2002**, *107*, art. no. 4014.
(92) Lawrence, J. R.; Nathanson, G. M. *Abstr. Pap. Am. Chem. Soc.* **2002**, *224*, 231-PHYS.
(93) Ringeisen, B. R.; Muenter, A. H.; Nathanson, G. M. *J. Phys. Chem. B* **2002**, *106*, 4999−5010.
(94) Torn, R. D.; Nathanson, G. M. *J. Phys. Chem. B* **2002**, *106*, 8064−8069.
(95) Finizio, A.; Mackay, D.; Bidleman, T.; Harner, T. *Atmos. Environ.* **1997**, *31*, 2289−2296.
(96) Gardner, J. A.; Watson, L. R.; Adewuyi, Y. G.; Davidovits, P.; Zahniser, M. S.; Worsnop, D. R.; Kolb, C. E. *J. Geophys. Res., Atmos.* **1987**, *92*, 10887−10895.
(97) Kolb, C. E.; Davidovits, P.; Jayne, J. T.; Shi, Q.; Worsnop, D. R. *Prog. React. Kinet. Mech.* **2002**, *27*, 1−46.
(98) Li, Y. Q.; Zhang, H. Z.; Davidovits, P.; Jayne, J. T.; Kolb, C. E.; Worsnop, D. R. *J. Phys. Chem. A* **2002**, *106*, 1220−1227.
(99) Zhang, H. Z.; Li, Y. Q.; Davidovits, P.; Williams, L. R.; Jayne, J. T.; Kolb, C. E.; Worsnop, D. R. *J. Phys. Chem. A* **2003**, *107*, 6398−6407.
(100) Zhang, H. Z.; Li, Y. Q.; Xia, J. R.; Davidovits, P.; Williams, L. R.; Jayne, J. T.; Kolb, C. E.; Worsnop, D. R. *J. Phys. Chem. A* **2003**, *107*, 6388−6397.
(101) Morris, J. W.; Davidovits, P.; Jayne, J. T.; Jimenez, J. L.; Shi, Q.; Kolb, C. E.; Worsnop, D. R.; Barney, W. S.; Cass, G. *Geophys. Res. Lett.* **2002**, *29*, art. no. 1357.
(102) Smith, G. D.; Woods, E.; DeForest, C. L.; Baer, T.; Miller, R. E. *J. Phys. Chem. A* **2002**, *106*, 8085−8095.
(103) Pradeep Kumar, P.; Broekhuizen, K.; Abbatt, J. P. D. *Atmos. Chem. Phys.* **2003**, *3*, 949−982.
(104) Cruz, C. N.; Pandis, S. N. *Environ. Sci. Technol.* **2000**, *34*, 4313−4319.
(105) Cruz, C. N.; Pandis, S. N. *Atmos. Environ.* **1997**, *31*, 2205−2214.
(106) Cruz, C. N.; Pandis, S. N. *J. Geophys. Res., Atmos.* **1998**, *103*, 13111−13123.
(107) Palm, W. U.; Millet, M.; Zetzsch, C. *Ecotox. Environ. Safe.* **1998**, *41*, 36−43.
(108) Folkers, M.; Mentel, T. F. Manuscript in preparation.
(109) Folkers, M. Proceedings of the American Geophysical Union Fall Meeting, San Francisco, 2002; Abstract A171F-103; p F106.
(110) Folkers, M.; Mentel, T. F.; Wahner, A. *Geophys. Res. Lett.* **2003**, in press.
(111) Vilan, A.; Ussyshkin, R.; Gartsman, K.; Cahen, D.; Naaman, R.; Shanzer, A. *J. Phys. Chem. B* **1998**, *102*, 3307−3309.

(112) Laux, J. M.; Fister, T. F.; FinlaysonPitts, B. J.; Hemminger, J. C. *J. Phys. Chem.* **1996**, *100*, 19891−19897.
(113) Luna, M.; Rieutord, F.; Melman, N. A.; Dai, Q.; Salmeron, M. *J. Phys. Chem. A* **1998**, *102*, 6793−6800.
(114) Peters, S. J.; Ewing, G. E. *Langmuir* **1997**, *13*, 6345−6348.
(115) Hu, J.; Xiao, X. D.; Ogletree, D. F.; Salmeron, M. *Science* **1995**, *268*, 267−269.
(116) Dai, Q.; Hu, J.; Freedman, A.; Robinson, G. N.; Salmeron, M. *J. Phys. Chem.* **1996**, *100*, 9−11.
(117) Trakhtenberg, S.; Naaman, R.; Cohen, S. R.; Benjamin, I. *J. Phys. Chem. B* **1997**, *101*, 5172−5176.
(118) Pankow, J. F. *Atmos. Environ.* **1994**, *28*, 189−193.
(119) Pankow, J. F. *Atmos. Environ.* **1994**, *28*, 185−188.
(120) Valsaraj, K. T.; Thoma, G. J.; Reible, D. D.; Thibodeaux, L. J. *Atmos. Environ.* **1993**, *27*, 203-210.
(121) Sagebiel, J. C.; Seiber, J. N. *Environ. Toxicol. Chem.* **1993**, *12*, 813−822.
(122) Luttke, J.; Levsen, K. *Atmos. Environ.* **1997**, *31*, 2649−2655.
(123) Cruz, C. N.; Dassios, K. G.; Pandis, S. N. *Atmos. Environ.* **2000**, *34*, 3897−3905.
(124) Shulman, M. L.; Charlson, R. J.; Davis, E. J. *J. Aerosol. Sci.* **1997**, *28*, 737−752.
(125) Lelieveld, J.; Crutzen, P. J. *J. Atmos. Chem.* **1991**, *12*, 229−267.
(126) Thornton, J.; Braban, C.; Abbatt, J. P. D. AGU 2003 abstract, 2003.
(127) Pankow, J. F. *J. Chromatogr.* **1991**, *547*, 488−493.
(128) Turpin, B. J.; Huntzicker, J. J.; Larson, S. M.; Cass, G. R. *Environ. Sci. Technol.* **1991**, *25*, 1788−1793.
(129) Fischer, R. G.; Kastler, J.; Ballschmiter, K. *J. Geophys. Res.* **2000**, *105*, 14473−14494.
(130) Obrien, J. M.; Shepson, P. B.; Muthuramu, K.; Hao, C.; Niki, H.; Hastie, D. R.; Taylor, R.; Roussel, P. B. *J. Geophys. Res.* **1995**, *100*, 22795−22804.
(131) Shepson, P. B.; Mackay, E.; Muthuramu, K. *Environ. Sci. Technol.* **1996**, *30*, 3618−3623.
(132) Kastler, J.; Ballschmiter, K. *Fresenius J. Anal. Chem.* **1998**, *360*, 812−816.
(133) Chuck, A. L.; Turner, S. M.; Liss, P. S. *Science* **2002**, *297*, 1151−1154.
(134) Nathanson, G. M.; Davidovits, P.; Worsnop, D. R.; Kolb, C. E. *J. Phys. Chem.* **1996**, *100*, 13007−13020.
(135) Davidovits, P.; Jayne, J. T.; Duan, S. X.; Worsnop, D. R.; Zahniser, M. S.; Kolb, C. E. *J. Phys. Chem.* **1991**, *95*, 6337−6340.
(136) Tsierkezos, N. G.; Molinou, I. E. *J. Chem. Eng. Data* **1998**, *43*, 989−993.
(137) Ammann, M.; Poschl, U.; Rudich, Y. *Phys. Chem. Chem. Phys.* **2003**, *5*, 351−356.
(138) Carslaw, K. S.; Peter, T. *Geophys. Res. Lett.* **1997**, *24*, 1743−1746.
(139) Tabazadeh, A.; Turco, R. P. *J. Geophys. Res., Atmos.* **1993**, *98*, 12727−12740.
(140) Jacobson, M. Z. *J. Geophys. Res., Atmos.* **1999**, *104*, 3527−3542.
(141) Arens, F.; Gutzwiller, L.; Baltensperger, U.; Gaggeler, H. W.; Ammann, M. *Environ. Sci. Technol.* **2001**, *35*, 2191−2199.
(142) Liu, S. C.; Trainer, M.; Fehsenfeld, F. C.; Parrish, D. D.; Williams, E. J.; Fahey, D. W.; Hubler, G.; Murphy, P. C. *J. Geophys. Res.* **1987**, *92*, 4191−4207.
(143) Rogge, W. F.; Hildemann, L. M.; Mazurek, M. A.; Cass, G. R.; Simonelt, B. R. T. *Environ. Sci. Technol.* **1991**, *25*, 1112−1125.
(144) Neeb, P.; Horie, O.; Moortgat, G. K. *J. Phys. Chem. A* **1998**, *102*, 6778−6785.
(145) Paulson, S. E.; Chung, M. Y.; Hasson, A. S. *J. Phys. Chem. A* **1999**, *103*, 8125−8138.
(146) Paulson, S. E.; Orlando, J. J. *Geophys. Res. Lett.* **1996**, *23*, 3727−3730.
(147) Atkinson, R. *J. Phys. Chem. Ref. Data* **1997**, *26*, 215−290.
(148) Atkinson, R. *Atmos. Environ.* **2000**, *34*, 2063−2101.
(149) Criegee, R. *Angew. Chem., Int. Ed.* **1975**, *14*, 745−752.
(150) Bailey, P. S. *Ozonation in Organic Chemistry*; Academic Press: New York, 1978.
(151) Finlayson-Pitts, B. J.; Pitts, J. N., Jr. *Chemistry of the Upper and Lower Atmosphere*; Academic Press: San Diego, 2000.
(152) Morrison, R. T.; Boyd, R. N. *Organic Chemistry*; Pentice Hall: Englewood Cliffs, NJ, 1992.
(153) Limbeck, A.; Puxbaum, H. *Atmos. Environ.* **1999**, *33*, 1847−1852.
(154) Kawamura, K.; Semere, R.; Imai, Y.; Fujii, Y.; Hayashi, M. *J. Geophys. Res., Atmos.* **1996**, *101*, 18721−18728.
(155) Kawamura, K.; Steinberg, S.; Kaplan, I. R. *Atmos. Environ.* **1996**, *30*, 1035−1052.
(156) Kawamura, K.; Yokoyama, K.; Fujii, Y.; Watanabe, O. *Geophys. Res. Lett.* **1999**, *26*, 871−874.
(157) Hurst, J.; Barket, D. J.; Shepson, P. B. *Environ. Sci. Technol.* **2003**, *37*, 2218−2225.
(158) Worsnop, D. R.; Morris, J. W.; Shi, Q.; Davidovits, P.; Kolb, C. E. *Geophys. Res. Lett.* **2002**, *29*, doi: 10.1029/2002GL015542.
(159) Pun, B. K.; Griffin, R. J.; Seigneur, C.; Seinfeld, J. H. *J. Geophys. Res.* **2002**, *107*, 4333, doi: 4310.1029/2001JD000542.
(160) Griffin, R. J.; Dabdud, D.; Seinfeld, J. H. *J. Geophys. Res.* **2002**, *107*, 4332, doi: 4310.1029/2001JD000541.
(161) Pankow, J. F.; Seinfeld, J. H.; Asher, W. E.; Erdakos, G. B. *Environ. Sci. Technol.* **2001**, *35*, 1164−1172.
(162) Lide, D. R. *CRC Handbook of Chemistry and Physics*, 78th ed.; CRC Press: Cleveland, 1998.
(163) Rudich, Y.; Talukdar, R. K.; Ravishankara, A. R. *J. Geophys. Res., Atmos.* **1996**, *101*, 21023-21031.
(164) Hanson, D. R.; Ravishankara, A. R.; Solomon, S. *J. Geophys. Res.* **1994**, *99*, 3615−3629.
(165) Spicer, C. W.; Chapman, E. G.; Finlayson-Pitts, B. J.; Plastridge, R. A.; Hubbe, J. M.; Fast, J. D.; Berkowitz, C. M. *Nature* **1998**, *394*, 353.
(166) Andrews, E.; Kreidenweis, S. M.; Penner, J. E.; Larson, S. M. *J. Geophys. Res., Atmos.* **1997**, *102*, 21997−22012.
(167) Novakov, T.; Hegg, D. A.; Hobbs, P. V. *J. Geophys. Res., Atmos.* **1997**, *102*, 30023−30030.
(168) Wasserman, S. R.; Tao, Y. T.; Whitesides, G. M. *Langmuir* **1989**, *5*, 1074−1087.
(169) Jayne, J. T.; Gardner, J. A.; Davidovits, P.; Worsnop, D. R.; Zahniser, M. S.; Kolb, C. E. *J. Geophys. Res.* **1990**, *95*, 20559−20563.
(170) Chu, L. T.; Leu, M. T.; Keyser, L. F. *J. Phys. Chem.* **1993**, *97*, 12798−12804.
(171) Remorov, R. G.; Gershenzon, Y. M.; Molina, L. T.; Molina, M. J. *J. Phys. Chem.*, in press.
(172) Clegg, S. M.; Abbatt, J. P. D. *Atmos. Chem. Phys.* **2001**, *1*, 73−78.
(173) Allanic, A.; Oppliger, R.; Rossi, M. J. *J. Geophys. Res.* **1997**, *102*, 23529−23541.
(174) Tabazadeh, A.; Toon, O. B.; Jensen, E. J. *Geophys. Res. Lett.* **1999**, *26*, 2211−2214.
(175) Hanson, D. R.; Ravishankara, A. R. *J. Phys. Chem.* **1994**, *98*, 5728−5735.
(176) Hanson, D. R. *J. Phys. Chem. B* **1997**, *101*, 4998.
(177) Schwartz, S. E. In *NATO ASI Ser.*; Jaeschke, W., Ed.; Springer-Verlag: New York, 1986; Vol. G6.
(178) Kubatova, A.; Vermeylen, R.; Claeys, M.; Cafmeyer, J.; Maenhaut, W.; Roberts, G.; Artaxo, P. *Atmos. Environ.* **2000**, *34*, 5037−5051.
(179) Stephanou, E. G.; Stratigakis, N. *Environ. Sci. Technol.* **1993**, *27*, 1403−1407.

CR020508F